

# A unified model of flames as gasdynamic discontinuities

By ANDREAS G. CLASS<sup>1</sup>, B. J. MATKOWSKY<sup>2</sup>  
AND A. Y. KLIMENKO<sup>3</sup>

<sup>1</sup>Institute for Nuclear and Energy Technologies, Forschungszentrum Karlsruhe GmbH,  
Karlsruhe, 76021, Germany

<sup>2</sup>Department of Engineering Sciences and Applied Mathematics, Northwestern University,  
Evanston, IL 60208, USA

<sup>3</sup>Department of Mechanical Engineering, The University of Queensland, Brisbane, Qld 4072, Australia

(Received 4 December 2001 and in revised form 6 February 2003)

Viewed on a hydrodynamic scale, flames in experiments are often thin so that they may be described as gasdynamic discontinuities separating the dense cold fresh mixture from the light hot burned products. The original model of a flame as a gasdynamic discontinuity was due to Darrieus and to Landau. In addition to the fluid dynamical equations, the model consists of a flame speed relation describing the evolution of the discontinuity surface, and jump conditions across the surface which relate the fluid variables on the two sides of the surface. The Darrieus–Landau model predicts, in contrast to observations, that a uniformly propagating planar flame is absolutely unstable and that the strength of the instability grows with increasing perturbation wavenumber so that there is no high-wavenumber cutoff of the instability. The model was modified by Markstein to exhibit a high-wavenumber cutoff if a phenomenological constant in the model has an appropriate sign. Both models are postulated, rather than derived from first principles, and both ignore the flame structure, which depends on chemical kinetics and transport processes within the flame. At present, there are two models which have been derived, rather than postulated, and which are valid in two non-overlapping regions of parameter space. Sivashinsky derived a generalization of the Darrieus–Landau model which is valid for Lewis numbers (ratio of thermal diffusivity to mass diffusivity of the deficient reaction component) bounded away from unity. Matalon & Matkowsky derived a model valid for Lewis numbers close to unity. Each model has its own advantages and disadvantages. Under appropriate conditions the Matalon–Matkowsky model exhibits a high-wavenumber cutoff of the Darrieus–Landau instability. However, since the Lewis numbers considered lie too close to unity, the Matalon–Matkowsky model does not capture the pulsating instability. The Sivashinsky model does capture the pulsating instability, but does not exhibit its high-wavenumber cutoff. In this paper, we derive a model consisting of a new flame speed relation and new jump conditions, which is valid for arbitrary Lewis numbers. It captures the pulsating instability and exhibits the high-wavenumber cutoff of all instabilities. The flame speed relation includes the effect of short wavelengths, not previously considered, which leads to stabilizing transverse surface diffusion terms.

---

## 1. Introduction

In unconfined premixed gaseous combustion, a mixture of fuel and oxidizer reacts in a flame to form the burned products. Sufficiently far ahead of and behind the

flame the composition and temperature of the gas, and consequently the density, are essentially constant. Since flames are typically thin compared with the characteristic scales of the fluid flow, a simplified model of premixed combustion views the flame as a surface of discontinuity separating the dense cold mixture from the light hot products. A model of this kind was first proposed independently by Darrieus (1938, 1945) and by Landau (1944). In the Darrieus–Landau model a flame propagating through a gaseous mixture is described by two incompressible fluids of different densities, separated by the flame surface. To complete the model it is necessary to provide an expression describing the evolution of the flame, e.g. the flame speed, and the relation between the fluid variables on either side of the flame. These, in fact, depend on the reaction kinetics and on transport processes within the flame. Rather than deriving these relations Darrieus and Landau postulated that the flame propagates normal to itself, at the fixed adiabatic flame speed  $\tilde{s}_F^0$  of a uniformly propagating planar flame. Thus, the flame speed  $\tilde{s}_F$  is

$$\tilde{s}_F = \tilde{s}_F^0. \quad (1.1)$$

Across the flame they postulated jump conditions which state that the mass and momentum fluxes are continuous across the flame. In non-dimensional form these relations are

$$[m] = 0, \quad [p + mv_n] = 0, \quad [\mathbf{v}_\perp] = 0, \quad (1.2)$$

where the square bracket denotes the jump of the indicated quantity across the flame surface,  $[*] = *_b - *_f$ , where  $*_b$  and  $*_f$  represent the quantity  $*$  evaluated at the flame surface as viewed from the burned and fresh gas, respectively. We will in general denote quantities referring to the burned and fresh gas by the subscripts  $b$  and  $f$ , respectively. Tildes denote dimensional quantities, while terms without a tilde are the corresponding non-dimensional quantities. Here,  $m = \tilde{m}/(\tilde{\rho}_f \tilde{s}_F^0)$ ,  $p = \tilde{p}/(\tilde{\rho}_f (\tilde{s}_F^0)^2)$ ,  $v_n = \tilde{v}_n/\tilde{s}_F^0$ , and  $\mathbf{v}_\perp = \tilde{\mathbf{v}}_\perp/\tilde{s}_F^0$  are the mass flux through the flame, the pressure, the normal velocity, and the tangential velocity, respectively. In terms of the density  $\rho = \tilde{\rho}/\tilde{\rho}_f$ , the normal velocity, and the normal speed of the flame relative to a fixed reference frame  $u_n = (\tilde{u}_n/\tilde{s}_F^0)$ , the mass flux is given by  $m = \rho(v_n - u_n)$ . The normal and tangential components of the velocity  $\mathbf{v} = \tilde{\mathbf{v}}/\tilde{s}_F^0$  are  $v_n = \mathbf{v} \cdot \mathbf{n}$  and  $\mathbf{v}_\perp = \mathbf{n} \times \mathbf{v} \times \mathbf{n}$ , respectively, where  $\mathbf{n}$  is the normal vector, pointing in the direction of the burned products. For the Darrieus–Landau model  $m \equiv 1$ . It is more common to describe the propagation of the flame in terms of the flame speed  $s_F = \tilde{s}_F/\tilde{s}_F^0$  which is defined as the relative speed of the flame with respect to the fresh mixture. In terms of the non-dimensional variables, with the fresh values taken as reference values,  $m = s_F = 1$ . A major problem with the Darrieus–Landau model is that planar flames propagating through a mixture initially at rest are unconditionally unstable to perturbations of any wavelength, in contradiction to laboratory observations. In order to overcome this deficiency of the Darrieus–Landau model, Markstein (1951, 1964) proposed a phenomenological model, where the flame speed is assumed to be proportional to the mean curvature  $\tilde{c} = -(\tilde{\nabla} \cdot \mathbf{n})/2$  of the flame,

$$\tilde{s}_F = \tilde{s}_F^0(1 - \tilde{l}_M 2\tilde{c}), \quad (1.3)$$

where  $\tilde{l}_M$  is the Markstein length which can be determined experimentally as in Searby & Quinard (1990). In non-dimensional terms,  $c = \tilde{c}\tilde{l}$  and  $\nabla = \tilde{l}\tilde{\nabla}$ , where  $\tilde{l}$  is a characteristic length scale of the flow (e.g. the diameter of a burner). Equation (1.3) can be written as

$$m = 1 - Mr 2c, \quad (1.4)$$

where the Markstein number  $Mr = \tilde{l}_M/\tilde{l}$ . In the Markstein model the jump conditions (1.2) are unchanged, and the dependence of the flame speed on curvature is postulated rather than derived from first principles. The Markstein length is a phenomenological quantity, unrelated to the physicochemical parameters of the mixture.

Following the ideas of Eckhaus (1961), Markstein (1964) generalized his earlier model to phenomenologically account for the curvature of the flow, i.e. the strain  $-\mathbf{n} \cdot \tilde{\nabla} \tilde{\mathbf{v}} \cdot \mathbf{n}$ , which yields

$$m = 1 - Mr(2c - \mathbf{n} \cdot \nabla \mathbf{v} \cdot \mathbf{n}). \quad (1.5)$$

This relation is in qualitative agreement with Karlovitz *et al.* (1953) who assumed that the flame speed depends not only on curvature but also on flame stretch  $\chi = \tilde{\chi}\tilde{l}/\tilde{s}_F^0$ , which is defined as the time derivative of the surface area of a flame element, normalized by the area itself. For uniformly propagating planar flames the Karlovitz stretch  $\chi$  is identical to the divergence of the tangential velocity, which for incompressible fluids is the strain  $-\mathbf{n} \cdot \nabla \mathbf{v} \cdot \mathbf{n}$ .

The theories of Darrieus–Landau, Markstein, and Karlovitz *et al.* are all phenomenological. That is, the authors did not derive their results from first principles: they did not consider the chemical reactions nor the transport processes occurring within the flame. Rather, the presence of the flame simply caused a jump in the density of the flow. In reality, the self-propagation mechanism of premixed flames is determined by a balance of chemical reactions, heat conduction, mass diffusion and convective transport of heat and species. In non-uniform time-dependent flows there is a strong interaction of the flow with this balance, resulting in a non-constant local flame propagation speed. In order to derive a model from first principles it is necessary to specify the chemical reactions and consider the internal structure of the flame. A characteristic scale for the thickness of the flame is  $\tilde{l}_0 = \tilde{\lambda}_f/(\tilde{s}_F^0 \tilde{\rho}_f \tilde{c}_{pf})$  where  $\tilde{\kappa}_f = \tilde{\lambda}_f/(\tilde{\rho}_f \tilde{c}_{pf})$  is the thermal diffusivity of the fresh mixture with the corresponding thermal conductivity  $\tilde{\lambda}_f$  and heat capacity  $\tilde{c}_{pf}$ . The ratio of the fluid scale to the flame thickness is the Péclet number  $Pe = \tilde{l}/\tilde{l}_0$ .

Barenblatt, Zeldovich & Istratov (1962) (see also Zeldovich *et al.*, Makhviladze 1985) introduced the diffusional thermal model of combustion. In contrast to the previously discussed purely hydrodynamic models, they ignored thermal expansion, but took into account transport processes and chemical reactions. In its simplest form the combustion process is considered as a one-step irreversible reaction between fuel and oxidizer. The reaction is deemed to have a high activation energy and is very sensitive to temperature variations so that the reaction is restricted to a thin zone, the reaction zone, near the maximum temperature. Mathematically, this property of the flames is expressed by a large value of the Zeldovich number  $Ze = \tilde{E}/(2\tilde{R}_g \tilde{T}_b)(1 - \tilde{T}_f/\tilde{T}_b)$ . Here  $\tilde{E}$  is the activation energy of the global reaction mechanism,  $\tilde{R}_g$  is the gas constant,  $\tilde{T}_f$  is the fresh temperature, and  $\tilde{T}_b$  is the adiabatic burned temperature of a uniformly propagating planar flame. The thickness of the reaction zone is  $O(\tilde{l}_0/Ze)$ . That is, the reaction zone is a thin layer  $O(1/Ze)$  within the flame zone. Behind the reaction zone there is no reaction since all the available fuel has been consumed in the reaction, while ahead of the reaction zone the reaction rate is negligibly small due to the low temperature. The preheat zone is located ahead of the reaction zone. Within the preheat zone, the mixture is preheated by conduction until reaction sets in at a sufficiently high temperature. In addition, within the preheat zone fuel diffuses toward the reaction zone where it is consumed. Due to the low thermal and mass

diffusivities of gas mixtures, the preheat zone is typically thin compared to the scale of the fluid flow.

The flame speed of premixed flames governed by a one-step irreversible reaction in a general fluid flow when thermal expansion is present is considered in several publications, e.g. Sivashinsky (1976), Clavin & Williams (1982), Matalon & Matkowsky (1982). The flame speed relation and the jump conditions are no longer postulated, but rather derived. In these models, the solution of the diffusional thermal problem, generalized to include the effects of thermal expansion, represents the thin flame structure which interacts with the flow on a larger scale, i.e. it is assumed that the flame curvature is weak compared to the thickness of the preheat zone, implying that variations along the flame are weak compared to variations normal to the flame. The flame characteristics depend on the Lewis number  $Le$ , defined as the ratio of thermal diffusivity to mass diffusivity of the limiting reaction component. The flame speed relation was derived by employing an asymptotic expansion in powers of  $Pe^{-1}$ . The models in Clavin & Williams (1982) and Matalon & Matkowsky (1982) provide perturbative corrections to the Darrieus–Landau model which are  $O(Pe^{-1})$ . The flame speed in Clavin & Williams (1982) is a linearization of the relation in Matalon & Matkowsky (1982), corresponding to the Clavin–Williams assumption of infinitesimal perturbations of nearly planar flames in nearly uniform flows.

Sivashinsky (1976) considered Lewis numbers not necessarily equal to unity. The jump conditions (1.2) are unchanged. The mass flux  $m$  is determined by

$$m^2 \ln m = Ze Pe^{-1} I_S \left( \frac{1}{m} \frac{\partial m}{\partial t} + \chi \right). \quad (1.6)$$

Here,  $t = \tilde{t} \tilde{s}_F^0 / \tilde{l}$  denotes time and  $I_S$  is a constant which depends on the properties of the mixture:

$$I_S = T_b \int_1^{T_b} \frac{\kappa(T)}{T} \left( 1 - \left( \frac{T-1}{T_b-1} \right)^{Le-1} \right) dT, \quad (1.7)$$

where  $\kappa(T) = \tilde{\lambda} \tilde{\rho}_f \tilde{c}_{pf} / (\tilde{\lambda}_f \tilde{\rho} \tilde{c}_p)$  is the thermal diffusivity as a function of temperature and  $T_b = \tilde{T}_b / \tilde{T}_f$  is the burned temperature. The mass flux, or flame speed, relation (1.6) is a nonlinear differential equation. However, Sivashinsky rejected the time-dependent relation (1.6) that he had derived because of stability considerations and considered (1.6) to be valid only for stationary flames.

Clavin & Williams (1982) considered infinitesimal perturbations of nearly planar flames in nearly uniform flows for near-equidiffusional flames, i.e.  $Le = 1 + o(1)$  with respect to an expansion in powers of  $Ze^{-1}$ . In this case the planar flame may be stable with respect to short-wavelength perturbations. The analysis in Clavin & Williams (1982) only yields the flame speed relation. Jump conditions for the case of infinitesimal perturbations of planar flames in nearly uniform flows were derived in Pelce & Clavin (1982), which provide perturbative corrections to the jump conditions in the Darrieus–Landau model, and represent a linearized version of the jump conditions in Matalon & Matkowsky (1982).

Matalon & Matkowsky (1982) considered arbitrary flame shapes for near-equidiffusional flames with thermal expansion in general flow fields. At leading order the model reduces to the Darrieus–Landau model. Including perturbative corrections, the mass flux through the flame becomes

$$m = 1 - Pe^{-1} \alpha_M \chi + O(Pe^{-2}), \quad (1.8)$$

$$\alpha_M = (T_b - 1)^{-1} T_b \ln T_b + Le_{\text{red}} I_M, \quad (1.9)$$

$$I_M(T_b) = \int_{-\infty}^0 \ln(1 + (T_b - 1)e^x) dx, \quad (1.10)$$

where  $Le_{\text{red}} = Ze(Le - 1)$  is the  $O(1)$  reduced Lewis number. The integral  $I_M$  depends on thermal expansion  $T_b - 1$  and  $\alpha_M$  is a physicochemical parameter which depends on thermal expansion, the Zeldovich number and the Lewis number. We note that the flame speed relation (1.8) is similar to the phenomenological relation (1.5), if we replace  $2c - \mathbf{n} \cdot \nabla \mathbf{v} \cdot \mathbf{n}$  by the stretch  $\chi$ . Indeed,  $2c - \mathbf{n} \cdot \nabla \mathbf{v} \cdot \mathbf{n}$  is the flame stretch of stationary flames. Therefore,  $Pe^{-1}\alpha_M$  can be identified as the Markstein number  $Mr$ , which is now given in terms of properties of the mixture, rather than being a phenomenological constant as originally proposed. As the mass flux relation now involves terms which are  $O(Pe^{-1})$  it is no longer sufficient to consider the jump conditions of Darrieus and Landau. They are replaced by the jump conditions of Matalon & Matkowsky (1982, 1984):

$$\left. \begin{aligned} [m] &= Pe^{-1}\chi \ln T_b + O(Pe^{-2}), \\ [p + mv_n] &= Pe^{-1}(T_b(T_b - 1)^{-1} \ln T_b [\nabla_n p] + 2c(T_b - 1 + T_b \ln T_b) \\ &\quad + u_n \chi \ln T_b) + O(Pe^{-2}), \\ [v_\perp] &= -Pe^{-1}(Pr + T_b(T_b - 1)^{-1} \ln T_b)[\mathbf{n} \times \nabla \times \mathbf{v}] + O(Pe^{-2}), \end{aligned} \right\} \quad (1.11)$$

where  $Pr$  is the Prandtl number and  $\nabla_n^* = \mathbf{n} \cdot \nabla^*$  is the normal derivative. The right-hand sides of (1.11) were explained as being due to transport along the flame.

Thus, at present there are separate theories for  $Le - 1 = O(1)$  (Sivashinsky 1976) and for  $Le \approx 1$  (Matalon & Matkowsky 1982). In Sivashinsky (1976) only the leading order term in the expansion in powers of  $Pe^{-1}$  is considered, while in Matalon & Matkowsky (1982),  $O(Pe^{-1})$  perturbative corrections are considered as well. A unified theory containing both cases is the goal of this paper. Moreover, in the unified theory we derive new expressions for the flame speed relation and jump conditions. In a companion paper, Class, Matkowsky & Klimenko (2003), the resulting model will be shown to be capable of capturing all the relevant instabilities of the planar flame, while eliminating non-physical short-wavelength instabilities present in the previous analyses.

Recently Klimenko & Class (2000) employed tensor calculus to derive the flame speed relations of the prior theories by Matalon & Matkowsky (1982) and Sivashinsky (1976) in a way that eliminates many of the purely geometrical terms which are present in the earlier works. In Klimenko & Class (2002) the approach was applied to a multistep chemical reaction. The nonlinear differential equation of Sivashinsky (1976) is replaced by a simpler algebraic relation. A coordinate system similar to that of Klimenko & Class (2000) was employed in De Goey & ten Thije Boonkkamp (1999).

In the present paper we employ a philosophy similar to that in Matalon & Matkowsky (1982) together with the tensor formalism of Klimenko & Class (2000) to derive new jump conditions and a new flame speed relation. Thus, we consider large Péclet numbers, effectively assuming that the flame, measured on the scale of the flame thickness is weakly curved. Our approach, though similar, differs somewhat from that of Matalon & Matkowsky (1982). Specifically, we consider both the equations which describe the reactive structure of the flame and those which govern the non-reactive hydrodynamic model. The solutions of both models must be identical away from the flame zone. Thus, equating the two models yields both the flame speed equation and

the jump conditions for the non-reactive hydrodynamic model. In the limit  $Pe \rightarrow \infty$  the reactive model is approximated by the hydrodynamic model, with the flame zone of the reactive model shrinking to the discontinuity surface of the hydrodynamic model, across which the fluid variables jump. The actual expressions for the jump conditions, as well as the flame speed relation, depend on the precise location of the discontinuity surface within the flame zone. Note that the discontinuity surface represents a mathematical construct rather than a physical surface of discontinuity and must be defined. Changing the location by  $O(Pe^{-1})$  induces  $O(Pe^{-1})$  changes in the flame speed relation and jump conditions. The fact that the form of the expression depends on the precise location of a separating surface was already recognized by Gibbs (1876 and 1878, 1879) when he considered the problem of surface tension on the surface separating two immiscible fluids. A flame position which is defined by a density integral is shown to be attractive as many of the terms in the jump conditions then vanish. The reason why these terms vanish is that the mass flux across the flame for this particular definition of the flame position becomes continuous. In the jump conditions for the normal momentum only a single correction term appears, which is proportional to the curvature of the flame. This term, due to compressibility effects, is analogous to the surface tension term in the problem of two immiscible fluids separated by an interface. However, its sign is opposite to that of surface tension. We therefore refer to it as surface compression. In the tangential momentum equations, the gradient of surface compression along the flame imposes tangential forces, analogous to the forces in the Marangoni convection problem.

In our approach we no longer consider  $Le \approx 1$  and  $Le - 1 = O(1)$  as separate cases. In addition, by accounting for the effects of short-wavelength variations along the flame, which were ignored in previous analyses, we derive a new flame speed relation. Short-wavelength effects result in new terms in the flame speed equation, which are not present in previous relations. In particular, we derive a transverse diffusion term and a nonlinear term involving transverse gradients. The transverse diffusion term plays a similar stabilizing role to that of the biharmonic operator in the Kuramoto–Sivashinsky equation (Sivashinsky 1980), which describes the weakly nonlinear evolution of flames in the constant-density approximation. The nonlinear term is similar to the nonlinear term in the Kuramoto–Sivashinsky equation, though the latter is due to a geometrical effect, while here it is due to transverse diffusion. If short wave variations are neglected our new flame speed relation reduces to the previous results of Matalon & Matkowsky (1982) and Sivashinsky (1976) in the appropriate limits. We also derive a new intermediate limit, in which the flame speed relation reduces to the stationary version of the Sivashinsky relation if we restrict consideration to corrugations of  $O(1)$  length scale and consider moderately large flame stretch. We also derive new expressions for the jump conditions.

The structure of the paper is as follows. In §2 the governing equations are presented and transformed to generalized moving coordinates. In §3 we introduce an asymptotic expansion in inverse powers of  $Pe$  and solve for the first two orders, which yields the fluid equations and the jump conditions. In §4 we derive the flame speed relation. Finally, in §5 the results are summarized and conclusions drawn.

## 2. Governing equations

The transport and reaction of a combustible mixture is governed by conservation equations for mass, momentum, energy, and the chemical species participating in the reaction. We consider a single deficient component of the reaction. We assume an

unconfined flame propagating at a speed much lower than the local sound speed. Thus, the Mach number  $Ma$  (ratio of flame speed to sound speed) is assumed to be small. Density changes are assumed to result from temperature changes only, i.e. we exclude acoustics from consideration. Compressibility effects are neglected in the energy equation as well.

In suitable non-dimensional variables the conservation equations for mass, momentum, energy and the deficient species concentration become

$$\frac{\partial R}{\partial t} + \nabla \cdot (RV) = 0, \quad (2.1)$$

$$\frac{\partial (RV)}{\partial t} + \nabla \cdot (RV \otimes V) = -\nabla P + \nabla \cdot \Sigma, \quad (2.2)$$

$$\frac{\partial (RT)}{\partial t} + \nabla \cdot (RVT) = \frac{1}{Pe} \nabla \cdot (\Lambda \nabla T) + (T_b - 1) W, \quad (2.3)$$

$$\frac{\partial (RY)}{\partial t} + \nabla \cdot (RVY) = \frac{1}{Pe Le} \nabla \cdot (\Lambda \nabla Y) - W. \quad (2.4)$$

We refer to this model as the reactive model. The equations correspond to the leading term in an expansion with respect to  $Ma^2$ . The quantity  $P$  in (2.2) corresponds to the deviation of the pressure from its constant ambient value, i.e. the pressure is  $P_0 + Ma^2 P$ , where the constant  $P_0$  does not enter the equations since only  $\nabla P$  appears.

We introduce a reference length  $\tilde{l}$  which is a characteristic length of the flow field. As a reference velocity we employ  $\tilde{s}_F^0$ , the adiabatic laminar flame speed. The thickness of the flame is estimated as  $\tilde{l}_0 = \tilde{\lambda}/(\tilde{\rho}_f \tilde{c}_{pf} \tilde{s}_F^0)$ . In atmospheric hydrocarbon combustion  $\tilde{l}_0 = O(0.1 \text{ mm})$ , while  $\tilde{l}$  is much larger. The ratio of the hydrodynamic length scale to the flame thickness is the Péclet number  $Pe = \tilde{l}/\tilde{l}_0$  which is assumed to be large. We use  $\tilde{T}_f$ ,  $\tilde{Y}_f$  and  $\tilde{\rho}_f$  as reference values for temperature, concentration and density. The transport coefficients are also non-dimensionalized by their fresh values.

The independent variables are the time  $t = \tilde{t} \tilde{s}_F^0 / \tilde{l}$  and the Cartesian spatial variables  $\eta_i = \tilde{\eta}_i / \tilde{l}$  ( $i = 1, 2, 3$ ). The nabla operator is  $\nabla = (\partial/\partial \eta_1, \partial/\partial \eta_2, \partial/\partial \eta_3)$  and the operator  $\otimes$  denotes the dyadic product.

Thus, the non-dimensional density, velocity, pressure, temperature, and deficient species concentration are  $R = \tilde{\rho}/\tilde{\rho}_f$ ,  $V = \tilde{v}/\tilde{s}_F^0$ ,  $P = \tilde{p}/(\tilde{\rho}_f (\tilde{s}_F^0)^2)$ ,  $T = \tilde{T}/\tilde{T}_f$ , and  $Y = \tilde{Y}/\tilde{Y}_f$ .

For convenience, we assume that there is a single species in the fresh mixture which is present in small quantity and which limits the reaction. This species is referred to as the deficient component. For lean (rich) hydrocarbon/air flames the deficient component is the hydrocarbon (oxygen). If a single deficient species is present it suffices to track this species. Other concentrations of the mixture are deemed to be sufficiently large that they can be considered essentially constant. Our approach may be generalized to more complex reaction schemes, in which case it is preferable to use the specific enthalpy of the mixture which is a function of the temperature, rather than the temperature itself. Typically, the specific heat  $\tilde{c}_p$  is only weakly dependent on the temperature in the temperature interval of interest. Thus, we replace  $\tilde{c}_p$  by its constant-temperature-averaged value.

Though the flow is incompressible outside the flame region, we must account for compressibility in the flame region. Thus, the stress tensor is given in the compressible form

$$\Sigma = Pr Pe^{-1} \Lambda (\nabla V + \nabla V^T - \frac{2}{3} I \nabla \cdot V), \quad (2.5)$$

where the superscript  $T$  denotes the transpose of the corresponding matrix and  $I$  denotes the identity matrix.

The quantity  $\Lambda = \tilde{\lambda}/\lambda_f$  is the non-dimensional thermal conductivity. From kinetic gas theory we find a theoretical dependence  $\Lambda \sim T^{1/2}$ . We assume that the diffusion coefficients for momentum, heat and species have the same temperature dependence but have distinct ratios, i.e. the Prandtl number  $Pr = \tilde{\mu}_f/(\tilde{\rho}_f\tilde{\kappa}_f)$  is the ratio of the kinematic viscosity  $\tilde{\mu}_f/\tilde{\rho}_f$  to the thermal diffusivity  $\tilde{\kappa}_f$  and the Lewis number  $Le = \tilde{\kappa}_f/\tilde{D}_f$  is the ratio of the thermal diffusivity to the species diffusivity  $\tilde{D}_f$ .

The temperature  $T$  and the density  $R$  are related by the equation of state, which for an ideal gas at constant ambient pressure is

$$TR = 1. \quad (2.6)$$

The reaction rate is given by the Arrhenius law  $W = AY^n \exp(-2ZeT_b/(T(1 - 1/T_b)))$ , where  $A$  is the pre-exponential factor,  $n$  is the reaction order,  $Ze$  is the Zeldovich number which is a non-dimensional measure of the activation energy. The adiabatic burned temperature is  $T_b = 1 + \tilde{Q}/(\tilde{c}_p\tilde{T}_f)$  where  $\tilde{Q}$  is the heat release of the reaction. We will employ the reaction sheet approximation corresponding to large  $Ze$ , i.e. we assume that the reaction rate  $W$  is highly sensitive to temperature changes. Thus, if the temperature becomes lower than the burned temperature  $T_b$  by a small amount the reaction rate decreases rapidly and may be neglected. Consequently, the reaction zone is thin compared to the thickness of the flame.

Note that if  $Le = 1$  the energy and concentration equations (2.3) and (2.4) become similar and the concentration and temperature are then related by  $(T - 1)/(T_b - 1) = 1 - Y$  so that a single equation describes the problem. Therefore, if  $Le$  is close to 1, the effect of the deviation of  $Le$  from unity represents an asymptotic correction and is manifested at the next order in the analysis. Thus, a correction to the leading order result is necessary if  $Le - 1$  is small, which is not the case if  $Le - 1 = O(1)$ . This previously required separate consideration of the cases  $Le - 1 = o(1)$  and  $Le - 1 = O(1)$ .

Here, the two cases are analysed together. We introduce the  $O(1)$  reduced enthalpy

$$H = \frac{1}{1 - Le^{-1}} \left( \frac{T - 1}{T_b - 1} + Y - 1 \right) \quad (2.7)$$

and write an equation for the enthalpy by dividing (2.3) by  $T_b - 1$ , adding (2.4), and then dividing the result by  $1 - Le^{-1}$  to yield

$$\frac{\partial(RH)}{\partial t} + \nabla \cdot (RVH) = \frac{1}{Pe} \nabla \cdot (\Lambda \nabla(H - Y)). \quad (2.8)$$

Note that  $H$  vanishes in the fresh mixture. The enthalpy equation (2.8) replaces the temperature equation (2.3). We will, however, employ (2.3) when we replace integration with respect to spatial variables by integration with respect to  $T$ .

To describe a propagating flame we must prescribe boundary conditions for the fluid variables as well as  $T = Y = 1$ ,  $H = 0$  far ahead of the flame and  $\nabla T = Y = \nabla H = 0$  far behind the flame, as well as appropriate initial conditions.

### 2.1. The hydrodynamic model

The flame is a layer separating the fresh mixture from the burned products. The density on either side of the layer is constant to the accuracy of the present theory but experiences a jump across the flame.



| Variable             | Hydrodynamic model    | Reactive model        |
|----------------------|-----------------------|-----------------------|
| density              | $\rho$                | $R$                   |
| velocity             | $\mathbf{v}, v^i$     | $\mathbf{V}, V^i$     |
| mass-flux            | $m^i$                 | $M^i$                 |
| pressure             | $p$                   | $P$                   |
| thermal conductivity | $\lambda$             | $\Lambda$             |
| stress               | $\boldsymbol{\sigma}$ | $\boldsymbol{\Sigma}$ |
| temperature          | $\vartheta$           | $T$                   |
| concentration        | $y$                   | $Y$                   |
| enthalpy             | $h$                   | $H$                   |
| reaction rate        |                       | $W$                   |

TABLE 1. Symbols in the hydrodynamic and the reactive models.

We propose to derive a hydrodynamic model for the flame. In the resulting model the internal structure of the flame, which is described by the reactive model, will not be resolved and is replaced by a discontinuity surface across which the variables of the hydrodynamic model jump from their fresh to their burned values. Note that the discontinuity surface represents a mathematical construct which must be properly defined. Sufficiently far ahead of and behind the flame, i.e. outside the layer, the hydrodynamic and the reactive models are identical. Therefore, differences between the two models may be observed within the flame structure only. Below we will consider the case where the hydrodynamic scale  $\tilde{l}$  is much larger than the flame thickness  $\tilde{l}_0$ , so that the layer represents an asymptotically thin inner layer embedded within the flow region of larger scale, i.e. the outer region.

The hydrodynamic model's parameters, such as the location of the discontinuity surface and the jump conditions across it, are determined from the internal structure of the flame. To derive the hydrodynamic model, we employ two sets of equations: one for the hydrodynamic model, and a second set for the reactive structure of the flame. Also note that both the reactive model and the hydrodynamic model are defined in the whole domain including the flame zone. We will choose the location of the discontinuity surface and derive the jump conditions and the flame speed relation. Finally, we consider the thin flame limit  $Pe \gg 1$  to derive explicit formulas for the flame speed relation and jump conditions.

To distinguish the variables of the hydrodynamic model from those of the reactive model we use lower-case letters for the former and capital letters for the latter. The variables in the reactive and hydrodynamic models are given in table 1 (some of the symbols are introduced in the sections that follow).

We also formulate the governing equations for the hydrodynamic model on either side of the flame as

$$\frac{\partial \rho}{\partial t} + \nabla \cdot (\rho \mathbf{v}) = 0, \quad (2.9)$$

$$\frac{\partial(\rho \mathbf{v})}{\partial t} + \nabla \cdot (\rho \mathbf{v} \otimes \mathbf{v}) = -\nabla p + \nabla \cdot \boldsymbol{\sigma}, \quad (2.10)$$

where  $\rho = \tilde{\rho}/\tilde{\rho}_f$ ,  $\mathbf{v} = \tilde{\mathbf{v}}/\tilde{v}_F^0$ , and  $p = \tilde{p}/(\tilde{\rho}_f(\tilde{v}_F^0)^2)$  are the density, velocity, and the dynamic pressure in the constant density flow. Here  $\boldsymbol{\sigma} = Pr Pe^{-1} \lambda (\nabla \mathbf{v} + \nabla \mathbf{v}^T - \frac{2}{3} \mathbf{I} \nabla \cdot \mathbf{v})$  is the stress tensor. The dynamic viscosity is given by the combination  $Pr Pe^{-1} \lambda$  where  $Re = Pe/Pr$  is the Reynolds number. In the fresh mixture  $\lambda = 1$ , while in the burned mixture  $\lambda = \lambda_b$ . In the burned region small variations of  $\lambda$  may result from

small temperature variations about the adiabatic temperature  $T_b$ . However, they will be shown to be negligibly small, so that  $\lambda_b = T_b^{1/2}$ .

In the hydrodynamic model the density  $\rho$  is constant both in the fresh and burned mixtures with  $\rho = \rho_f = 1$  and  $\rho = \rho_b = 1/T_b$ . Behind the flame the small variations of the temperature  $\vartheta$  about  $T_b$ , i.e. small variations of the enthalpy  $h$  about zero, result in small variations of the density  $\rho$  so that  $\rho - \rho_b = O(\vartheta - T_b) = O(h(1 - Le^{-1}))$ . This difference is shown to be negligible. Thus, in the hydrodynamic model the densities ahead of and behind the flame are constant but different.

The hydrodynamic model concentration  $y$  is uniform in both the fresh and the burned regions, where the concentrations are 1 and 0, respectively.

Clearly, the equations of the reactive and hydrodynamic models are nearly identical. Yet, there is an important difference. The hydrodynamic model holds separately on either side of the flame and does not include a reaction term, while the reactive model governs all the processes within the flame structure.

To close the hydrodynamic model the effects of flame structure on the non-reactive flow on either side of the flame must be accounted for. These result in jumps in the density, mass flux and momentum flux across the discontinuity surface, which must be determined. In addition, the speed of the discontinuity surface must be determined.

The goal of the analysis that follows is to derive from first principles the jump conditions across the discontinuity surface and the flame speed relation.

## 2.2. Jump conditions

Instead of using fixed Cartesian coordinates it is convenient to transform the equations to a moving generalized curvilinear coordinate system  $x^1, x^2, x^3$  where  $x^1 = 0$  specifies the discontinuity surface, which has been referred to as the flame surface. The coordinate system is chosen such that in the normal direction it is attached to the discontinuity surface and in the tangential direction it moves with the local tangential flow. Thus, in this coordinate system the flame is at rest with no flow along the flame surface. In our analysis we employ tensor calculus (see Aris 1989). Without loss of generality the  $x^1$  coordinate lines can be chosen to be normal to the surfaces  $x^1 = \text{const}$  including the discontinuity surface  $x^1 = 0$ . The covariant metric tensor for this system of coordinates is given by  $g^{ij}$  ( $i, j = 1, 2, 3$ ). Due to the orthogonality of the  $x^1$  coordinate lines with respect to the surfaces  $x^1 = \text{const}$ ,  $g^{1\alpha} = 0$  where Greek indices run from 2 to 3 and Latin indices run from 1 to 3. Without loss of generality we set  $g^{11} = 1$ , i.e. the normal coordinate is uniformly spaced (see Klimenko & Class 2000). We use lower-case letters for the spatial variables and the metric tensor, as we did for the hydrodynamic model variables. This emphasizes the fact that in the asymptotic theory for thin flames that follows, the metric tensor is constant to leading order within the flame region. Quantities which vary on the large hydrodynamic scale are denoted by lower-case letters while functions which vary within the flame structure are denoted by capital letters. We introduce the volume element  $\sqrt{g}$  where  $g \equiv 1/\det(g^{ij})$ , which is identical to the element of surface area since  $g^{11} = 1$ . This allows us to define the mean curvature  $c$  of the surface  $x^1 = 0$  by  $c = -(\partial \sqrt{g}/\partial x^1)/(2\sqrt{g})$  evaluated at  $x^1 = 0$ .

Note that in tensor notation the physical components of vectors and tensors are calculated from contravariant/covariant components using the normalization

$$V(i) = V^i \sqrt{g_{ii}} = V_j g^{ij} \sqrt{g_{ii}}, \quad \text{no summation on } i, \quad (2.11)$$

$$\Sigma(ij) = \Sigma^{ik} g_{jk} \sqrt{g_{ii}/g_{jj}}, \quad \text{no summation on } i, j, \quad (2.12)$$

where  $V(i)$  and  $\Sigma(ij)$  denote physical components, while the quantities on the right-hand side are the corresponding tensor components. The covariant matrix tensor  $g_{ij}$  is the inverse of the matrix  $g^{ij}$ .

Consider the conservation equation for a scalar quantity  $\Phi$  in fixed Cartesian space

$$\frac{\partial}{\partial t}(\Phi) + \nabla \cdot (\mathbf{J}(\Phi)) = Pe Q(\Phi), \quad (2.13)$$

where  $\mathbf{J}(\Phi) = \mathbf{V}\Phi - D\nabla\Phi$ , with velocity  $\mathbf{V}$  and diffusivity  $D$ , is the flux associated with  $\Phi$  and  $Q(\Phi)$  is a source term, scaled by the Péclet number for convenience.

In generalized moving coordinates the conservation equation for  $\Phi$  is written in terms of conventional derivatives as

$$\frac{\partial}{\partial t}(\sqrt{g}\Phi) + \frac{\partial}{\partial x^j}(\sqrt{g}J^j(\Phi)) = \sqrt{g}Pe Q(\Phi), \quad (2.14)$$

where we employ the Einstein summation convention of summing repeated indices. The flux vector becomes  $J^j(\Phi) = (V^j - u^j)\Phi - g^{ij}D\partial\Phi/\partial x^i$  where  $u^j \equiv \partial x^j/\partial t$  is the speed of the moving  $x^j$ -system of coordinates relative to the fixed  $\eta^j$ -system of coordinates.

We decompose summation with respect to the index  $j$  in (2.14) into its normal and tangential components

$$\frac{\partial}{\partial t}(\sqrt{g}\Phi) + \frac{\partial}{\partial x^1}(\sqrt{g}J^1(\Phi)) + \frac{\partial}{\partial x^\alpha}(\sqrt{g}J^\alpha(\Phi)) = \sqrt{g}Pe Q(\Phi). \quad (2.15)$$

A conservation equation for the volume element  $\sqrt{g}$  is obtained if we consider the transport equation for  $\Phi = 1$  and neither allow for diffusion ( $D=0$ ) nor a source term ( $Q(1)=0$ ), so that the corresponding flux results from convection of the coordinate system alone,  $J^j(1) = -u^j$ . The resulting equation is used in the definition of flame stretch.

We now write the fluxes and source terms for each of the governing equations. The fluxes of the continuity ( $\Phi = R$ ), energy ( $\Phi = RT$ ), concentration ( $\Phi = RY$ ), and enthalpy ( $\Phi = H$ ) equations are

$$J^j(R) \equiv M^j, \quad (2.16)$$

$$J^j(RT) \equiv M^j T - \frac{1}{Pe} g^{ij} \Lambda \frac{\partial T}{\partial x^i}, \quad (2.17)$$

$$J^j(RY) \equiv M^j Y - \frac{1}{Pe Le} g^{ij} \Lambda \frac{\partial Y}{\partial x^i}, \quad (2.18)$$

$$J^j(RH) = M^j H - \frac{1}{Pe} g^{ij} \Lambda \frac{\partial}{\partial x^i}(H - Y), \quad (2.19)$$

where  $M^j = R(V^j - u^j)$  is the contravariant mass flux in the moving system of coordinates and the corresponding source terms are

$$Q(R) = Q(H) \equiv 0, \quad Q(RT) \equiv (T_b - 1)W, \quad Q(RY) \equiv -W. \quad (2.20)$$

Since momentum is a vector quantity, the momentum equations are not in the appropriate form to apply (2.15). However, if we write a scalar momentum conservation equation in a fixed spatial direction we may apply (2.15). We introduce a parallel vector field  $l_i$ , which in Cartesian coordinates has constant components, i.e. has constant direction and length, and write the conservation equation for  $V^i l_i$ , which represents the velocity component in the direction of  $l_i$ . A parallel vector field has special properties with respect to differentiation. In particular, covariant derivatives, denoted by  $(\cdot)_{,i}$ , which are the tensorial generalization of partial derivatives, of parallel

vector fields vanish, i.e.  $l_{i,j} = 0$ . For a moving coordinate system, as considered here, this is true at any instant of time. However, the components of  $l_i$  are time dependent. The metric tensor has a similar property (Ricci's lemma), i.e.  $g^{ij}_{,k} = 0$ . In the following analysis we will need the relation  $\partial l_1 / \partial x^1 = 0$  which follows from Ricci's lemma,  $g^{1\alpha} = 0$ , and  $g^{11} = 1$ :

$$g_{,i}^{11} = \frac{\partial g^{11}}{\partial x^i} + 2\Gamma_{ij}^1 g^{1j} = 2\Gamma_{i1}^1 = 0, \quad (2.21)$$

$$g_{,1}^{1\alpha} = \frac{\partial g^{1\alpha}}{\partial x^1} + \Gamma_{j1}^1 g^{\alpha j} + \Gamma_{1j}^\alpha g^{1j} = \Gamma_{11}^\alpha = 0, \quad (2.22)$$

where  $\Gamma_k^{ij}$  are Christoffel symbols of the second kind. Now we calculate  $l_{1,1}$  to find that it vanishes since  $l_1$  is a parallel vector:

$$l_{1,1} = \frac{\partial l_1}{\partial x^1} - \Gamma_{11}^i l_i = \frac{\partial l_1}{\partial x^1} = 0. \quad (2.23)$$

The momentum equation is obtained if we set

$$J^j(RV^i l_i) \equiv (M^j V^i + g^{ij} P - \Sigma^{ij}) l_i, \quad Q(RV^i l_i) \equiv 0, \quad (2.24)$$

where the stress tensor is

$$\Sigma^{ij} = \frac{Pr}{Pe} \Lambda \left( g^{jk} \frac{\partial V^i}{\partial x^k} + g^{ik} \frac{\partial V^j}{\partial x^k} - V^k \frac{\partial g^{ij}}{\partial x^k} - \frac{2}{3} \frac{g^{ij}}{\sqrt{g}} \frac{\partial \sqrt{g} V^k}{\partial x^k} \right). \quad (2.25)$$

Flux equations for the hydrodynamic model are obtained by replacing the reactive model variables by the corresponding hydrodynamic model variables:

$$J^j(\rho) \equiv m^j, \quad Q(\rho) \equiv 0, \quad (2.26)$$

$$J^j(\rho v^i l_i) \equiv (m^j v^i + g^{ij} p - \sigma^{ij}) l_i, \quad Q(\rho v^i l_i) \equiv 0, \quad (2.27)$$

$$J^j(\rho y) \equiv m^j y - \frac{1}{Le Pe} g^{ij} \lambda \frac{\partial y}{\partial x^i}, \quad Q(\rho y) \equiv 0, \quad (2.28)$$

$$J^j(\rho h) \equiv m^j h - \frac{1}{Pe} g^{ij} \lambda \frac{\partial h}{\partial x^i}, \quad Q(\rho h) \equiv 0, \quad (2.29)$$

where all the source terms vanish in the hydrodynamic model. The stress tensor is

$$\sigma^{ij} = \frac{Pr}{Pe} \lambda \left( g^{jk} \frac{\partial v^i}{\partial x^k} + g^{ik} \frac{\partial v^j}{\partial x^k} - v^k \frac{\partial g^{ij}}{\partial x^k} - \frac{2}{3} \frac{g^{ij}}{\sqrt{g}} \frac{\partial \sqrt{g} v^k}{\partial x^k} \right). \quad (2.30)$$

Henceforth, we denote  $m^1$  at the discontinuity surface by  $m$ , to be consistent with the notation in the introduction. This is appropriate since  $g^{11} = 1$  so that the physical normal mass flux  $m$  equals the corresponding mass flux  $m^1$  in tensor notation:

$$m = m^1|_{x^1=0}. \quad (2.31)$$

Let us examine the difference between the equations for the reactive and the hydrodynamic model. These equations only differ by the fact that in the hydrodynamic model the variables jump while in the reactive model there is a continuous variation and a reaction term. In particular, density is constant on either side of the discontinuity surface in the hydrodynamic model, while in the reactive model the density varies continuously. Outside the reaction layer there is no reaction. Thus, both models describe the same non-reactive hydrodynamic flow so that there is no density difference between the two.

From the continuity equations we obtain

$$\frac{\partial}{\partial t}(\sqrt{g}(R - \rho)) + \frac{\partial}{\partial x^\alpha}(\sqrt{g}(M^\alpha - m^\alpha)) + \frac{\partial}{\partial x^1}(\sqrt{g}(M^1 - m^1)) = 0. \quad (2.32)$$

We will now apply a simple procedure to determine the jump conditions for the hydrodynamic model. We note that this procedure differs from the procedure used in matched asymptotics. Here, we use the fact that the hydrodynamic and reactive models describe the same non-reactive flow outside the flame zone, i.e. both models are identical far from the discontinuity surface. At this stage, our procedure is applicable even when the reaction layer is not thin within the flame. We note that when we finally apply the asymptotic limit below, we are able to calculate asymptotic corrections to the jump conditions without the need to determine asymptotic corrections to the solutions in the flame zone, which is the most complicated step in the traditional approach. At this stage we make no assumptions on the reaction scheme and the fluid properties, so that the results we obtain are general.

Integrating equation (2.32) across the fresh mixture from  $x^1 = x_f^1 < 0$  to  $x^1 = 0$  (the discontinuity surface) and across the burned region from  $x^1 = 0$  to  $x^1 = x_b^1 > 0$  and summing the integrals yields

$$\frac{\partial}{\partial t} \left( \int_{x_f^1}^{x_b^1} \sqrt{g}(R - \rho) dx^1 \right) + \frac{\partial}{\partial x^\alpha} \left( \int_{x_f^1}^{x_b^1} \sqrt{g}(M^\alpha - m^\alpha) dx^1 \right) + \sqrt{g}^* [m] = 0, \quad (2.33)$$

where  $x_f^1$  is sufficiently far upstream that reaction and heat conduction from the flame are negligible. Similarly,  $x_b^1$  is sufficiently far downstream that reaction is negligible. The square bracket  $[m]$  denotes the jump of the hydrodynamic model's normal mass flux  $m$ , i.e.  $m^1$  at the discontinuity surface. This term is sometimes referred to as the excess surface mass. The term arises from the normal mass flux in (2.32). Both at  $x^1 = x_f^1$  and  $x^1 = x_b^1$  the reactive and the hydrodynamic model mass fluxes are identical so that no contributions are found at the upstream ( $x^1 = x_f^1$ ) and downstream ( $x^1 = x_b^1$ ) integration boundaries. At the discontinuity surface ( $x^1 = \pm 0$ ) the reactive model mass flux  $M^1$  is continuous, so that the corresponding terms cancel each other. The asterisk denotes quantities evaluated at the discontinuity surface. It should be noted that we have written the sum of the integrals in the fresh and the burned mixtures as a single integral. In an actual evaluation the density  $\rho$  must be replaced by the fresh density  $\rho_f$  in  $x^1 \in (x_f^1, 0)$  and by the burned density  $\rho_b$  in  $x^1 \in (x_b^1, \infty)$ . Note that (2.33) is the jump condition for the mass flux  $m$ . However, it is necessary to evaluate the integrals in (2.33) which involve the reactive model which must be analysed.

The relation (2.33) suggests that the hydrodynamic model mass flux may be discontinuous at the discontinuity surface. This will be discussed below. However, we will define the precise location of the discontinuity surface in such a way that  $m$  is continuous across this surface. Rather than defining the location of the discontinuity surface as the surface of maximum reaction rate as has been done previously and then evaluating the corresponding excess surface mass, we now choose the location of the discontinuity surface such that the excess surface mass vanishes. This may be ensured if each integral in (2.33) separately vanishes. Both integrals involve terms which may be adjusted. The transverse mass fluxes  $M^\alpha$  and  $m^\alpha$  both contain the transverse speed  $u^\alpha$  of the coordinate system, which is as yet undetermined. The transverse speed  $u^\alpha$  can always be chosen to ensure both that the coordinate lines  $x^1$  remain

orthogonal to the surfaces  $x^1 = \text{const}$  and that the integral  $\int_{x_f^1}^{x_b^1} \sqrt{g}(M^\alpha - m^\alpha) dx^1 = 0$ . This requires that  $M^\alpha = R(V^\alpha - u^\alpha) \approx 0$  and  $m^\alpha = \rho(v^\alpha - u^\alpha) \approx 0$ , i.e. the coordinate system is transported along the flame approximately at the speed of the tangential flow. Note that we cannot enforce  $M^\alpha = m^\alpha = 0$ , since the tangential mass fluxes change weakly within the flame structure and also  $M^\alpha \neq m^\alpha$ . This will be clarified below when we asymptotically approximate the integrals. The integral involving the time derivative in (2.33) may be made to vanish by choosing an appropriate position for the discontinuity surface. This too will be clarified below. The requirement that  $\int_{-\infty}^{\infty} \sqrt{g}(R - \rho) dx^1 = 0$  will determine the position of the discontinuity surface.

A jump condition similar to (2.33) is derived from the hydrodynamic and the reactive model momentum equations (2.15) with the corresponding fluxes defined in (2.24) and (2.27). Again the difference of the equations is taken and then the equation integrated across the reactive structure to yield

$$\begin{aligned} & \frac{\partial}{\partial t} \left( \int_{x_f^1}^{x_b^1} \sqrt{g} (RV^i l_i - \rho v^i l_i) dx^1 \right) \\ & + \frac{\partial}{\partial x^\alpha} \left( \int_{x_f^1}^{x_b^1} \sqrt{g} (J^\alpha(RV^i l_i) - J^\alpha(\rho v^i l_i)) dx^1 \right) + \sqrt{g}^* [J^1(\rho v^i l_i)] = 0. \end{aligned} \quad (2.34)$$

The jump  $[J^1(\rho v^i l_i)] = [mv^i + g^{i1}p - \sigma^{i1}]l_i^*$  involves the terms which are present in the Darrieus–Landau jump conditions and, in addition, the jump of the stress across the discontinuity surface. In order to satisfy continuity of the normal mass flux  $m^1$  across the flame we have used all the degrees of freedom at our disposal. Therefore, we must expect that the integral in (2.34) does not vanish. Thus, forces must be associated with the discontinuity surface, which account for compressibility effects within the flame structure.

Repeating our procedure for the enthalpy equation yields

$$\begin{aligned} & \frac{\partial}{\partial t} \left( \int_{x_f^1}^{x_b^1} \sqrt{g}(RH - \rho h) dx^1 \right) \\ & + \frac{\partial}{\partial x^\alpha} \left( \int_{x_f^1}^{x_b^1} \sqrt{g} (J^\alpha(RH) - J^\alpha(\rho h)) dx^1 \right) + \sqrt{g}^* [J^1(\rho h)] = 0, \end{aligned} \quad (2.35)$$

where  $[J^1(\rho h)] = m_b^{j*} h_b^* - Pe^{-1} \lambda_b^* (\partial h_b / \partial x^1)_b^*$  and where the asterisk and the subscript  $b$  denote quantities evaluated at the discontinuity surface as seen from the burned mixture.

Finally, repeating our procedure for the concentration, we determine the equation for the propagation speed of the discontinuity surface.

$$\begin{aligned} & \frac{\partial}{\partial t} \left( \int_{x_f^1}^{x_b^1} \sqrt{g}(RY - \rho y) dx^1 \right) + \frac{\partial}{\partial x^\alpha} \left( \int_{x_f^1}^{x_b^1} \sqrt{g} (J^\alpha(RY) - J^\alpha(\rho y)) dx^1 \right) \\ & - \sqrt{g}^* m = Pe \int_{x_f^1}^{x_b^1} \sqrt{g} Q(RY) dx^1, \end{aligned} \quad (2.36)$$

where we employed  $[J^1(\rho y)] = m(y_b - y_f) = -m$ . Note that the source term  $Q(RY)$  depends on the temperature and thus on the enthalpy  $h_b^*$ . Thus, both (2.35) and (2.36) must be solved to calculate the flame speed.

In the analysis to follow we determine the appropriate position of the discontinuity surface and its normal propagation speed. In addition, the jump conditions for the mass and momentum are derived.

### 3. Asymptotic derivation of the fluid equations and jump conditions

In §2.2 we derived the jump conditions for mass (2.33), momentum (2.34), enthalpy (2.35), and concentration (2.36) which arise upon replacing the flame region by a surface across which the fluid variables jump. In the hydrodynamic model enthalpy and concentration no longer appear. Instead an equation for the propagation of the discontinuity surface is derived from (2.35)–(2.36). To explicitly determine expressions for the fluid jump conditions and the flame speed relation it will be necessary to asymptotically evaluate the integrals in (2.33)–(2.36). We derive asymptotic formulas taking advantage of the fact that flames are typically thin compared to the length scale of the fluid flow, i.e.  $Pe^{-1} \ll 1$ . We will see that the integrals are  $O(Pe^{-1})$ .

We are interested in the flame zone, which is thin. In the terminology of matched asymptotics the flame region represents an inner region embedded within the outer non-reactive flow. Within the flame zone there is the yet thinner reaction zone. We introduce the stretched normal spatial variable  $X = Pe x^1$ . In terms of  $X$  the width of the flame region is  $O(1)$  and the integration boundaries  $x_f^1$  and  $x_b^1$  become  $X = -\infty$  and  $X = \infty$ , respectively.

Equation (2.15) becomes

$$\frac{1}{Pe} \left( \frac{\partial}{\partial t} (\sqrt{g} \Phi) + \frac{\partial}{\partial x^\alpha} (\sqrt{g} J^\alpha(\Phi)) \right) + \frac{\partial}{\partial X} (\sqrt{g} J^1(\Phi)) = \sqrt{g} Q(\Phi). \quad (3.1)$$

We now exploit the fact that  $Pe \gg 1$ . Note that  $Ze^{-1} = o(1)$  in an expansion in powers of  $Pe^{-1}$ . We expand as

$$F \sim \sum_n Pe^{-n} F_{(n)}, \quad (3.2)$$

where  $F$  denotes any of the reactive model quantities  $R$ ,  $T$ ,  $Y$ ,  $H$ ,  $W$ ,  $P$ ,  $V^i$ ,  $M^i$ ,  $J^j(R)$ ,  $J^j(RT)$ ,  $J^j(RY)$ ,  $J(RH)$ ,  $J^j(RV^i l_i)$ , and  $\Sigma^{ij}$ .

Quantities associated with the coordinate system  $\sqrt{g}$ ,  $g^{ij}$ ,  $c$ , and its speed  $u^i$ , as well as the parallel vector field  $l_i$  are Taylor expanded as

$$f = \sum_{n=0} \frac{\partial^n f(0)}{(\partial x^1)^n} \frac{Pe^{-n}}{n!} X^n = \sum_{n=0} Pe^{-n} f_{(n)}^* X^n, \quad (3.3)$$

where  $f$  denotes any of the quantities  $\sqrt{g}$ ,  $g^{ij}$ ,  $c$ ,  $u^i$ , and  $l_i$ . The coefficients  $f_{(n)}^*$  are independent of  $X$ , though they may vary along the flame. The hydrodynamic model quantities  $\rho$ ,  $p$ ,  $v^i$ ,  $m^i$ ,  $h$ ,  $J^j(\rho)$ ,  $J^j(\rho v^i l_i)$ ,  $J(\rho h)$  and  $\sigma^{ij}$  may jump at  $X=0$ , or at least their normal derivatives may jump, so that we Taylor expand these quantities separately in the fresh and burned regions.

Introducing the Taylor expansion  $g^{1/2} = g_{(0)}^{1/2*} + Pe^{-1} g_{(1)}^{1/2*} X + \dots$  into (3.1), where  $g_{(1)}^{1/2*} = -2c$  and  $\chi^* = (\partial g^{1/2*} / \partial t) / g^{1/2*}$ , yields

$$\begin{aligned} \frac{1}{Pe} \left( \left( \frac{\partial}{\partial t} + \chi^* \right) \Phi + \frac{1}{\sqrt{g}^*} \frac{\partial}{\partial x^\alpha} (\sqrt{g}^* J^\alpha(\Phi)) \right) + \frac{\partial}{\partial X} \left( \left( 1 - \frac{1}{Pe} 2cX \right) J^1(\Phi) \right) \\ = \left( 1 - \frac{1}{Pe} 2cX \right) Q(\Phi) + O(Pe^{-2}). \end{aligned} \quad (3.4)$$

Note that we have omitted the index (0) for convenience in Taylor-expanded quantities evaluated at the discontinuity surface. Substituting the asymptotic expansions for the fluxes and the source terms into (3.4) and setting the coefficients of like powers of  $Pe^{-1}$  to zero yields

$$\frac{\partial}{\partial X} (J_{(0)}^1(\Phi)) = Q_{(0)}(\Phi), \quad (3.5)$$

$$\begin{aligned} \left(\frac{\partial}{\partial t} + \chi^*\right) \Phi_{(0)} + \frac{1}{\sqrt{g^*}} \frac{\partial}{\partial x^\alpha} (\sqrt{g^*} J_{(0)}^\alpha(\Phi)) + \frac{\partial}{\partial X} (J_{(1)}^1(\Phi) - 2cX J_{(0)}^1(\Phi)) \\ = Q_{(1)}(\Phi) - 2cX Q_{(0)}(\Phi). \end{aligned} \quad (3.6)$$

Similarly, we write two terms of the asymptotic expansion of a generic jump condition

$$[J_{(0)}^1(\phi)] = \int_{-\infty}^{\infty} Q_{(0)}(\Phi) dX, \quad (3.7)$$

$$\begin{aligned} [J_{(1)}^1(\phi)] = \int_{-\infty}^{\infty} (Q_{(1)}(\Phi) - 2cX Q_{(0)}(\Phi)) dX - \left(\frac{\partial}{\partial t} + \chi^*\right) \int_{-\infty}^{\infty} (\Phi_{(0)} - \phi_{(0)}) dX \\ - \int_{-\infty}^{\infty} \frac{1}{\sqrt{g^*}} \frac{\partial}{\partial x^\alpha} (\sqrt{g^*} (J_{(0)}^\alpha(\Phi) - J_{(0)}^\alpha(\phi))) dX. \end{aligned} \quad (3.8)$$

Here  $\phi$  denotes a generic variable of the hydrodynamic model and  $\Phi$  denotes the corresponding variable of the reactive model.

Note that  $\chi^*$  is the relative change of the element of surface area (since  $g^{11} = 1$ ). This quantity is related to the flame stretch  $\chi$ . Indeed, we will show that these quantities are identical in our moving coordinate system since there is no flow on the flame surface. For now, we distinguish between  $\chi^*$  and the stretch  $\chi$ . The quantities  $\chi^*$ ,  $c$ , and  $u^j$  are related by the conservation equation for the volume element  $g^{1/2}$ , i.e.  $\Phi = 1$ . Equation (3.6) with  $\partial u^1 / \partial X = 0$  yields

$$\chi^* = \frac{1}{\sqrt{g^*}} \frac{\partial}{\partial x^\alpha} (\sqrt{g^*} u_{(0)}^\alpha) - 2cu_{(0)}^1, \quad (3.9)$$

where the normal speed of the coordinate system  $u^1$  may be expressed in terms of the mass flux as  $u_{(0)}^{1*} = v_f^{1*} - m_{(0)} = v_b^{1*} - m_{(0)}/\rho_b^*$ . Clearly, there is a contribution to  $\chi^*$  due to tangential velocity gradients (first term on the right-hand side of (3.9)) and a second contribution due to curvature (second term on the right-hand side of (3.9)).

The leading terms (3.5) and (3.6) of the asymptotic expansion of (3.4) are expressed in terms of conventional derivatives, so that (3.5) and (3.6) may be employed directly, without resorting to tensor calculus. The equations explicitly involve the flame stretch  $\chi$  and the flame curvature  $c$  as parameters. Therefore, employing (3.5) and (3.6) directly yields the solutions in terms of  $\chi$  and  $c$ . Both parameters represent intrinsic geometric properties of the flame surface. Specifically,  $\chi$  represents temporal surface area changes and  $c$  measures the current shape of the flame. We use the term *intrinsic disturbed flame equations* for (3.5) and (3.6), as in Klimenko & Class (2000) where the energy equation and the concentration equation were introduced in a form similar to (3.4). Similarly, we introduce the term *intrinsic disturbed flame jump conditions* for (3.7) and (3.8). However, since short-wave perturbations of the flame were neglected in Klimenko & Class (2000), but are considered here, the transverse derivative does not appear in Klimenko & Class (2000). For the momentum equations, which were not considered in Klimenko & Class (2000), the transverse derivative term in (3.6)



also cannot be neglected and represents an essential part of the *intrinsic disturbed flame equations*.

We derived the first two terms (3.5), (3.6), in an asymptotic expansion of the intrinsic disturbed flame equations. From the leading-order equations we first derive the leading-order solution and jump conditions. From the  $O(Pe^{-1})$  equations we then derive perturbative corrections of the jump conditions and also the flame speed relation for unsteady flames of general shape.

### 3.1. Leading-order fluid equations and jump conditions

At leading order the fresh and burned densities are  $\rho_{f(0)} = 1$  and  $\rho_{b(0)} = 1/T_b$ .

The fluid equations have no source term  $Q(\Phi)$ . Thus, the leading-order equation (3.5) implies that the normal fluxes  $J_{(0)}^1(\Phi)$  are independent of the normal coordinate  $X$ :

$$m_{f(0)}^1 = \text{const}, \quad J_{f(0)}^1(\rho v^i l_i) = \text{const}, \quad (3.10)$$

$$m_{b(0)}^1 = \text{const}, \quad J_{b(0)}^1(\rho v^i l_i) = \text{const}, \quad (3.11)$$

$$M_{(0)}^1 = \text{const}, \quad J_{(0)}^1(RV^i l_i) = \text{const}. \quad (3.12)$$

Applying the intrinsic disturbed flame jump condition (3.7) implies that at leading order the normal fluxes do not jump and thus are constant within the flame region,

$$M_{(0)}^1 = m_{f(0)}^1 = m_{b(0)}^1 \equiv m_{(0)}, \quad (3.13)$$

$$J_{(0)}^1(RV^i l_i) = J_{f(0)}^1(\rho v^i l_i) = J_{b(0)}^1(\rho v^i l_i) = J_{(0)}^{1*}(\rho v^i l_i). \quad (3.14)$$

In order to be consistent with the notation in the introduction we write  $m_{(0)}$  for the normal mass flux at the discontinuity surface rather than  $m_{(0)}^{1*}$ . Though there are no variations across the flame zone, variations in the tangential direction are permitted.

We summarize this result by writing the leading-order jump conditions (2.33) and (2.34) for the hydrodynamic model:

$$[m_{(0)}] = 0, \quad (3.15)$$

$$[m_{(0)} v_{(0)}^i + g^{i1*} p_{(0)}] l_i^* = 0. \quad (3.16)$$

Since the parallel vector field is arbitrary, the momentum jump must hold separately for the normal and tangential components, i.e.

$$[m_{(0)} v_{(0)}^1 + p_{(0)}] = 0, \quad (3.17)$$

$$[m_{(0)} v_{(0)}^\alpha] = 0, \quad \text{so that } [v_{(0)}^\alpha] = 0. \quad (3.18)$$

Note that these are exactly the jump conditions that appear in the Darrieus–Landau model. The last relation states that the tangential velocity is continuous across the flame so that  $v_{f(0)}^\alpha = v_{b(0)}^\alpha = v_{(0)}^{\alpha*}$ . Employing the definitions of the mass fluxes in the hydrodynamic and reactive models,  $M^i = R(V^i - u^i)$  and  $m^i = \rho(v^i - u^i)$ , respectively, yields the normal velocities

$$V_{(0)}^1 = m_{(0)}/R_{(0)} + u_{(0)}^{1*}, \quad v_{f(0)}^1 = m_{(0)} + u_{(0)}^{1*}, \quad v_{b(0)}^1 = m_{(0)}/\rho_{b(0)}^* + u_{(0)}^{1*}, \quad (3.19)$$

so that the jump of the hydrodynamic model normal velocity is  $[v_{(0)}^1] = m_{(0)}[1/\rho_{(0)}]$ .

Since we employ a coordinate system which is convected along the flame with the local tangential flow velocity, i.e.

$$v_{(0)}^{\alpha*} = u_{(0)}^{\alpha*}, \quad (3.20)$$

the hydrodynamic model tangential mass flux vanishes in both the fresh and burned mixtures,  $m_{f(0)}^\alpha = m_{b(0)}^\alpha = m_{(0)}^{\alpha*} = 0$ . In our coordinate system the flame element is identical to the element of surface area  $g^{1/2*}$  so that the flame stretch at leading order is

$$\chi = \chi^* = \frac{1}{\sqrt{g^*}} \frac{\partial \sqrt{g^*}}{\partial t}. \quad (3.21)$$

Now, employing the definitions of  $J^1(RV^i l_i)$  and  $J^1(\rho v^i l_i)$  given by (2.24) and (2.27), as well as (3.14) which states that the fluxes are identical, yields

$$m_{(0)}(V_{(0)}^1 l_1^* + V_{(0)}^\alpha l_\alpha^*) + l_1^* P_{(0)} - Pr \Lambda_{(0)} \left( \frac{\partial V_{(0)}^\alpha}{\partial X} l_\alpha^* + \frac{4}{3} \frac{\partial V_{(0)}^1}{\partial X} l_1^* \right) = J_{(0)}^{1*}(\rho v^i l_i), \quad (3.22)$$

$$m_{(0)}(v_{(0)}^1 l_1^* + v_{(0)}^\alpha l_\alpha^*) + l_1^* p_{(0)} = J_{(0)}^{1*}(\rho v^i l_i), \quad (3.23)$$

where  $\partial V_{(0)}^1 / \partial X = m_{(0)} \partial (1/R_{(0)}) / \partial X$ . Note that we have decomposed summation on the repeated index  $i$ , into its normal ( $i = 1$ ) and tangential contributions ( $i = \alpha = 2, 3$ ). Subtracting (3.22) from (3.23) and equating the terms which multiply the tangential component of  $l_\alpha^*$  yields

$$0 = m_{(0)}(v_{(0)}^{\alpha*} - V_{(0)}^\alpha) + Pr \Lambda_{(0)} \frac{\partial V_{(0)}^\alpha}{\partial X}. \quad (3.24)$$

Solutions of this equation that match the solution in the fresh region have the form

$$V_{(0)}^\alpha = v_{(0)}^{\alpha*} + B \exp(Pr^{-1} m_{(0)} \zeta), \quad \zeta = \int_0^X \frac{1}{\Lambda_{(0)}} dX, \quad (3.25)$$

where the constant  $B$  is chosen to yield the appropriate behaviour as  $X \rightarrow \infty$ , i.e. in the non-reactive burned region. Exponentially growing solutions must be excluded as they grow without bound. Thus, the tangential velocity is constant at leading order:

$$V_{(0)}^\alpha = v_{(0)}^{\alpha*}. \quad (3.26)$$

Substituting this into the definition of the reactive model tangential mass flux yields

$$M_{(0)}^\alpha = R_{(0)}(v_{(0)}^{\alpha*} - u_{(0)}^\alpha) = 0. \quad (3.27)$$

Subtracting (3.23) from (3.22) and equating the terms which multiply the normal component of  $l_1^*$  yields

$$P_{(0)} - p_{(0)} = m_{(0)} \left( \frac{4}{3} Pr \Lambda_{(0)} \frac{\partial}{\partial X} \left( \frac{1}{R_{(0)}} \right) + m_{(0)} \left( \frac{1}{\rho_{(0)}} - \frac{1}{R_{(0)}} \right) \right). \quad (3.28)$$

This relation determines the difference between the pressure in the two models (discontinuous pressure in the hydrodynamic model and continuous pressure in the reactive model).

Finally, we calculate the tangential fluxes  $J^\alpha(RV^i l_i)$  and  $J^\alpha(\rho v^i l_i)$  defined in (2.24) and (2.27) as

$$J_{(0)}^\alpha(RV^i l_i) = \left( P_{(0)} + \frac{2}{3} Pr \Lambda_{(0)} \frac{\partial V_{(0)}^1}{\partial X} \right) g^{\alpha\beta*} l_\beta^*, \quad (3.29)$$

$$J_{(0)}^\alpha(\rho v^i l_i) = p_{(0)} g^{\alpha\beta*} l_\beta^*. \quad (3.30)$$

Note that there is no term involving  $l_1^*$  in (3.29) and (3.30). After eliminating the pressure using (3.28), we have

$$J_{(0)}^\alpha(RV^i l_i) - J_{(0)}^\alpha(\rho v^i l_i) = m_{(0)} \Pi g^{\alpha\beta} l_\beta^*, \quad (3.31)$$

where

$$\Pi = 2Pr A_{(0)} \frac{\partial}{\partial X} \left( \frac{1}{R_{(0)}} \right) + m_{(0)} \left( \frac{1}{\rho_{(0)}} - \frac{1}{R_{(0)}} \right), \quad (3.32)$$

which defines the difference between the tangential momentum fluxes in the reactive and hydrodynamic models.

In this section we derived solutions to the leading-order flow equations and jump conditions. The leading-order solution is independent of the flame curvature and flame stretch and does not involve time derivatives. Therefore, the leading-order solution corresponds to a steadily propagating planar flame, except that the leading-order flame speed has not yet been determined. The leading-order solution enters the  $O(Pe^{-1})$  equations where the effects of unsteadiness, curvature and stretch are accounted for and therefore must be determined before these effects can be properly accounted for.

### 3.2. $O(Pe^{-1})$ fluid equations and jump conditions

At this order we are not interested in the profiles of the variables within the flame region. We merely wish to determine perturbative corrections to the jump conditions of the flow variables. The intrinsic disturbed flame jump condition (3.8) for the mass flux yields

$$\left( \frac{\partial}{\partial t} + \chi \right) I_R + [m_{(1)}] = 0, \quad (3.33)$$

where we have used  $M_{(0)}^\alpha = m_{(0)}^\alpha = Q(R) = 0$ , and introduced

$$I_R = \int_{-\infty}^0 (R_{(0)} - \rho_{f(0)}) dX + \int_0^\infty (R_{(0)} - \rho_{b(0)}) dX. \quad (3.34)$$

Below, we will choose the location for the discontinuity surface by requiring that  $I_R = 0$ . Similarly, the intrinsic disturbed flame jump condition (3.8) for the momentum is

$$\begin{aligned} & \left( \frac{\partial}{\partial t} + \chi \right) \left( l_i^* \int_{-\infty}^\infty (R_{(0)} V_{(0)}^i - \rho v_{(0)}^i) dX \right) \\ & + \frac{1}{\sqrt{g^*}} \frac{\partial}{\partial x^\alpha} \int_{-\infty}^\infty \sqrt{g^*} (J_{(0)}^\alpha(RV^i l_i) - J_{(0)}^\alpha(\rho v^i l_i)) dX + [J_{(1)}^i(\rho v^i l_i)] = 0. \end{aligned} \quad (3.35)$$

From  $M_{(0)}^j - m_{(0)}^j = 0$ , it follows that  $R_{(0)} V_{(0)}^i - \rho v_{(0)}^i = u_{(0)}^{i*} (R_{(0)} - \rho_{(0)})$ , so that the first integral can be expressed in terms of  $I_R$ . Employing (3.31) simplifies the second integral so that

$$[J_{(1)}^i(\rho v^i l_i)] + \left( \frac{\partial}{\partial t} + \chi \right) (u_{(0)}^{i*} l_i^* I_R) + \frac{1}{\sqrt{g^*}} \frac{\partial}{\partial x^\alpha} (\sqrt{g^*} g^{\alpha\beta} l_\beta^* m_{(0)} I_\sigma) = 0, \quad (3.36)$$

where  $I_\sigma = \int_{-\infty}^0 \Pi_f dX + \int_0^\infty \Pi_b dX$ . Since we will chose  $I_R \equiv 0$  below, we can write  $I_\sigma = I_\sigma + a I_R$  where  $a$  is an arbitrary constant. In particular, we may select  $a = -m_{(0)} T_b$  where the kernels of the integrals ahead of and behind the flame become identical

and thus can be written as a single integral:

$$I_\sigma - m_{(0)}T_b I_R = 2Pr \int_1^{T_b} T^{1/2} dT + m_{(0)} \int_{-\infty}^{\infty} (T-1)(T_b/T-1) dX, \quad (3.37)$$

where we have employed  $\Lambda = T^{1/2}$  and the ideal gas law. Obviously  $I_\sigma - m_{(0)}T_b I_R$  is positive as the kernels of the integrals are positive.

Since  $l_j$  is a parallel vector, the divergence of the vector  $g^{ji}l_j = l^i$  vanishes, i.e.

$$0 = \frac{1}{\sqrt{g}} \frac{\partial}{\partial x^i} (\sqrt{g} g^{ji} l_j) = \frac{1}{\sqrt{g}} \frac{\partial}{\partial x^\alpha} (\sqrt{g} g^{\alpha\beta} l_\beta) + \frac{1}{\sqrt{g}} \frac{\partial}{\partial x^1} (\sqrt{g} g^{11} l_1), \quad (3.38)$$

where  $1/\sqrt{g} \partial(\sqrt{g} g^{11} l_1)/\partial x^1 = -2cl_1$  since  $g^{11} = 1$  and  $\partial l_1/\partial x^1 = 0$  as shown in (2.23).

Perturbative corrections of the normal momentum flux, defined in (2.27), may be expanded as

$$[J_{(1)}^1(\rho v^i l_i)] = [m_{(0)}v_{(1)}^i + m_{(1)}v_{(0)}^i + g^{i1*} p_{(1)} - \sigma_{(1)}^{i1}] l_i^*. \quad (3.39)$$

Substituting (3.38) and (3.39) into (3.36) finally yields the perturbative corrections of the momentum jump conditions

$$\begin{aligned} & [m_{(0)}v_{(1)}^i + m_{(1)}v_{(0)}^i + g^{i1*} p_{(1)} - \sigma_{(1)}^{i1}] l_i^* \\ & = -\left(\frac{\partial}{\partial t} + \chi\right) (u_{(0)}^{i*} l_i^* I_R) - \left(2cl_1 + g^{\alpha\beta*} l_\beta^* \frac{\partial}{\partial x^\alpha}\right) m_{(0)} I_\sigma. \end{aligned} \quad (3.40)$$

The momentum jump condition (3.40) yields the momentum jump in the direction of  $l_i^*$ , which is arbitrary. The right-hand side results from compressibility effects inside the flame. It is not trivial to decompose this jump condition into its normal and tangential contributions since  $\partial l_i^*/\partial t$  is non-zero as the discontinuity surface propagates and deforms. Moreover, both  $I_R$  and  $I_\sigma$  depend on the precise location of the discontinuity surface. Below, we use relation (3.33) to define the precise location of the discontinuity surface by requiring that each term in (3.33) vanishes. Then, we decompose the momentum jump condition (3.40) into normal and tangential jump conditions.

### 3.3. Flame location

The hydrodynamic model mass flux exhibits  $O(Pe^{-1})$  variations within the flame zone which depend on the curvature  $c$  and on the flame stretch  $\chi$ . The slope of the mass flux is in general different on either side of the surface as the densities differ. There is, however, a specific location where the hydrodynamic model mass fluxes in the fresh and burned mixture are identical, though not equal to the reactive model mass flux at this location. Figure 1(a) shows this schematically. The solid line indicates the reactive model mass flux, while the dashed and the dotted lines indicate the hydrodynamic model mass flux in the fresh and burned mixtures (and their continuations), respectively. Also shown is the reaction zone. The difference between the heights of the hydrodynamic model mass flux curves corresponds to the jump in the mass flux across the flame, i.e. the excess surface mass. If we use the intersection of the hydrodynamic model mass flux curves as the definition of the flame surface position, then the excess surface mass vanishes so that the mass flux is continuous at the discontinuity surface, though its slope is discontinuous. The flame position where  $[m] = 0$  is determined from equation (3.33) and requires that the integral  $I_R$  defined

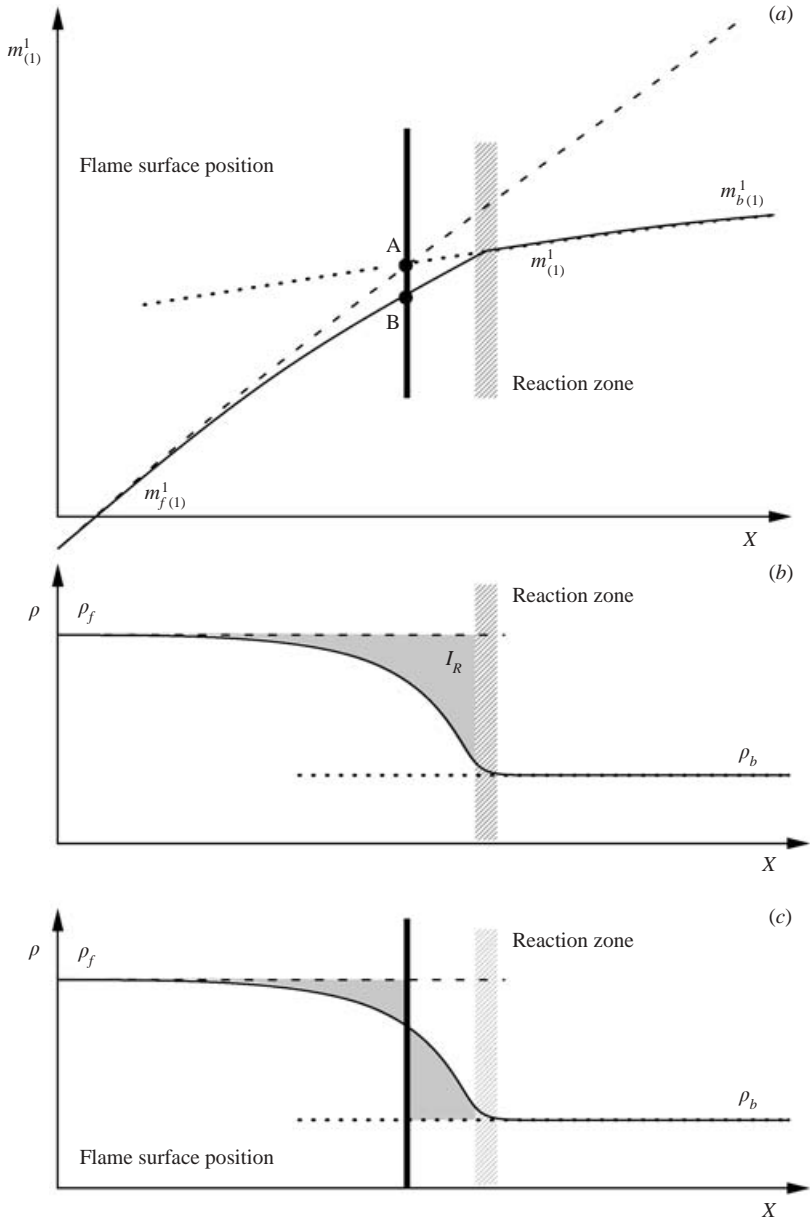


FIGURE 1. (a) Definition of the flame surface position from the intersection of the hydrodynamic model mass fluxes. (b, c) The density integral  $I_R$  for two different flame positions ((b) surface located at reaction zone, (c) surface located to yield continuous mass flux).

by (3.34) vanishes:

$$I_R = \int_{-\infty}^0 (R_{(0)} - \rho_{f(0)}) dX + \int_0^{\infty} (R_{(0)} - \rho_{b(0)}) dX \equiv 0. \quad (3.41)$$

Note that  $I_R \neq 0$  for other choices of the flame surface location. Figure 1(b, c) shows this schematically. Again, the solid line indicates the reactive model's continuous density, the dashed line indicates the fresh density and the dotted line indicates

the burned density. In Figure 1(b) the reaction zone is chosen as the flame surface position, so that the reactive model density is larger than the hydrodynamic model density throughout the preheat zone and the integral  $I_R$  corresponds to the shaded region. In Figure 1(c) the flame surface position is chosen according to relation (3.41). Now the hydrodynamic model density is larger than the reactive model density ahead of the flame surface position and vice versa behind. The shaded regions correspond to the difference between the two models solutions. Here, the areas of the two shaded regions are identical so that the integral  $I_R$  vanishes.

To calculate  $\chi$  without employing our special coordinate system in which  $g^{11} = 1$ , we use  $g^{11} = |\nabla T|^2$  instead. Then, employing

$$\mathbf{u}_{(0)} = \mathbf{n} \times \mathbf{V} \times \mathbf{n} - \frac{\partial T}{\partial t} \frac{1}{|\nabla T|} \mathbf{n} + o(1) \quad (3.42)$$

and replacing  $\sqrt{g^*}$  in (3.9) by  $\sqrt{g} \sqrt{g^{11}}$  yields a formula for the flame stretch:

$$\chi = \frac{1}{\sqrt{g^*}} \frac{\partial(\sqrt{g^*} u_{(0)}^j)}{\partial x^j} \Big|_{x^1=0} = \frac{1}{\sqrt{g^{11}g}} \frac{\partial(\sqrt{g^{11}g} u_{(0)}^j)}{\partial x^j} \Big|_{x^1=0} = \frac{1}{|\nabla T|} \nabla \cdot (|\nabla T| \mathbf{u}_{(0)}) \Big|_{T=T^*}, \quad (3.43)$$

which can easily be evaluated. Here,  $T^*$  is the temperature at the discontinuity surface.

Note that at the flame surface there is a difference between the reactive model mass flux (point B in figure 1a) and the hydrodynamic model mass flux (point A in figure 1a) which we derive. The difference may be calculated as

$$M_{(1)}^{1*} - m_{(1)} = \left( \frac{\partial}{\partial t} + \chi \right) \int_0^\infty (R_{(0)} - \rho_{b(0)}) dX = - \left( \frac{\partial}{\partial t} + \chi \right) \int_{-\infty}^0 (R_{(0)} - \rho_{f(0)}) dX. \quad (3.44)$$

After combining the results from the leading order and  $O(Pe^{-1})$  we find

$$m = M^{1*} - \left( \frac{\partial}{\partial t} + \chi \right) \int_0^\infty (R - \rho_b) dx^1 + O(Pe^{-2}). \quad (3.45)$$

The difference  $M^{1*} - m$  between the normal mass flux in the hydrodynamic model ( $m$ ) and the reactive model mass flux ( $M^{1*}$ ) is proportional to the density integral  $\int_0^\infty (R - \rho_b) dx^1$  which itself is proportional to the thickness of the flame. The thickness of the flame depends on the current flame speed, so that time derivatives of the integral are mainly due to changes of the flame speed. Also, the difference  $M^{1*} - m$  is proportional to flame stretch. Note that the integral  $\int_0^\infty (R - \rho_b) dx^1$  is small as the flame is thin so that the difference  $M^{1*} - m$  is  $O(Pe^{-1})$ .

In §2.2 we derived the jump condition for the normal mass flux (2.33). We defined the location of the discontinuity surface such that the excess surface mass vanishes so that the normal mass flux is continuous across the discontinuity surface. For thin flames, relation (3.41) allows us to explicitly calculate the precise location of the flame front which ensures continuous normal mass flux across the flame. We describe how the location of the discontinuity surface and how the normal mass flux through the discontinuity surface may be calculated. We also provide a simple formula to calculate the flame stretch at the discontinuity surface.

We next consider the reaction sheet approximation, in which the flame position can be determined explicitly.

### 3.3.1. Flame location in the reaction sheet approximation

The flame location is determined by the requirement that  $I_R$ , which is an integral over the spatial variable, vanishes. We note that if the flame speed changes by  $O(1)$ , the spatial profiles of the fluid variables also change by  $O(1)$ . However, in the reaction sheet approximation, typical of combustion, it is possible to convert integrals with respect to space into integrals with respect to temperature, which allows us to explicitly determine the flame location as a function of temperature.

At leading order, the intrinsic disturbed flame equation (3.5) requires that the normal flux  $J_{(0)}^1(RT)$  given by (2.17) is independent of  $X$ , i.e.  $J_{(0)}^1(RT) = \text{const}$ , where the constant is readily determined from the fresh mixture, so that we have

$$m_{(0)}T_{(0)} - \Lambda_{(0)} \frac{\partial T_{(0)}}{\partial X} = m_{(0)}. \quad (3.46)$$

We may now calculate the integrals  $I_R$  and  $I_\sigma$ , given as functions of  $X$ , in terms of the temperature using the relation

$$dX = \frac{\Lambda_{(0)}}{m_{(0)}} \frac{dT_{(0)}}{(T_{(0)} - 1)}. \quad (3.47)$$

For an ideal gas the density is  $R = 1/T$  and the conductivity is  $\Lambda = T^{1/2}$ . Employing (3.47) in the condition for the flame surface position (3.41) yields

$$\begin{aligned} 0 &= \int_1^{T_{(0)}^*} T^{-1/2} dT - \frac{1}{T_b} \int_{T_{(0)}^*}^{T_b} T^{-1/2} \frac{T_b - T}{T - 1} dT \\ &= 2/T_b (\sqrt{T_b} - T_b + (T_b - 1) (\sqrt{T_{(0)}^*} + \tanh^{-1} \sqrt{T_b} - \tanh^{-1} \sqrt{T_{(0)}^*})) \end{aligned} \quad (3.48)$$

which may be solved for the temperature  $T_{(0)}^*$  which defines the position of the discontinuity surface.

Equation (3.48) is independent of the normal mass flux  $m_{(0)}$ , so that the discontinuity surface is an isotherm  $T = T_{(0)}^*$  of the reactive model. We note that in the conventional definition the temperature at the flame surface is near the burned temperature  $T_b$ , while our definition, based on fluid mechanical considerations, leads to a flame surface located at a position where the temperature is lower.

This has a significant effect on the flame speed relation. This becomes obvious if we consider a flame subjected to strong flame stretch, a case beyond the validity of our model, but nevertheless instructive. Consider a planar flame stabilized in a symmetric opposed-jet configuration. Here, the plane of symmetry represents a stagnation plane where the normal flow vanishes. For strong stagnation point flow, i.e. strong flame stretch, the reaction zone may move to the opposite side of the stagnation plane. The conventional definition of the flame speed, based on the maximum reaction rate, results in a negative flame speed. In contrast, our definition of the flame position (3.34), which defines the flame speed as the mass burning rate at a position where the temperature is only weakly elevated, ensures a positive flame speed. The flame speed relation shows a much weaker dependence on the flame stretch compared to the conventional definition.

We now compute the integral  $I_\sigma$  in (3.37) which arises in the perturbative  $I_\sigma$  correction of the momentum jump condition (3.40). Employing (3.47) and  $I_R = 0$  we find

that

$$I_\sigma = \int_1^{T_b} T^{1/2} (2Pr + T_b/T - 1) dT = \frac{4}{3}(Pr + 1)(T_b^{3/2} - 1) - 2(T_b - 1). \quad (3.49)$$

The integral  $I_\sigma > 0$  vanishes for constant-density flow, i.e.  $T_b = 1$ , and  $I_\sigma$  strongly grows with increasing thermal expansion.

### 3.4. Fluid equations and jump conditions in the reaction sheet approximation

The flow ahead of and behind the flame is governed by equations (2.9) and (2.10), which are the incompressible Navier–Stokes equations. The flow fields are related by a set of jump conditions across the flame. In contrast to the Darrieus–Landau jump conditions, the jump conditions now include  $O(Pe^{-1})$  corrections.

In the hydrodynamic model a surface of discontinuity, a mathematical construct, replaces the continuous flame structure. We choose this surface based on the requirement that  $I_R = 0$ . Due to our definition of the flame surface position the jump conditions (3.33) and (3.40) simplify substantially compared to the jump conditions obtained using a different flame surface position, e.g. Matalon & Matkowsky (1982). Moreover, we also consider the effect of  $m_{(0)} - 1 = O(1)$ , i.e. flame speeds which differ by  $O(1)$  from the propagation speed of a uniformly propagating planar flame when  $Le$  is not near unity. This results in new terms in the jump conditions, not present in Matalon & Matkowsky (1982). We combine the leading-order jump conditions (3.15) and (3.16) with the perturbative corrections (3.33) and (3.40). Furthermore, we decompose the jump condition for the momentum vector into its normal and tangential components. This can be done easily if we set the arbitrary parallel vector  $l_i^*$  equal to the normal or tangential vector. Since  $I_R = 0$  the time derivatives of  $l_i^*$ , which make the decomposition complicated, are no longer present. We obtain

$$[m] = 0, \quad (3.50)$$

$$[mv^1 + p - \sigma^{11}] = -Pe^{-1}2cmI_\sigma + o(Pe^{-1}), \quad (3.51)$$

$$[mv^\alpha - \sigma^{1\alpha}] = -Pe^{-1}g^{\alpha\beta*} \frac{\partial}{\partial x^\beta} (mI_\sigma) + o(Pe^{-1}). \quad (3.52)$$

In the coordinate-free form described in the introduction,  $v_n = \mathbf{v} \cdot \mathbf{n}$  and  $\mathbf{v}_\perp = \mathbf{n} \times \mathbf{v} \times \mathbf{n}$  correspond to  $v^1$  and  $v^\alpha$ , respectively, so that the momentum jumps are

$$[mv_n + p - \sigma_{nn}] = -Pe^{-1}2cmI_\sigma + o(Pe^{-1}), \quad (3.53)$$

$$[m\mathbf{v}_\perp - \boldsymbol{\sigma}_{n\perp}] = -Pe^{-1}\nabla_\perp(mI_\sigma) + o(Pe^{-1}). \quad (3.54)$$

Here, the tangential derivative is  $\nabla_\perp(\cdot) = \mathbf{n} \times \nabla(\cdot) \times \mathbf{n}$ , and the stresses  $\sigma_{nn}$  and  $\sigma_{n\perp}$  at the discontinuity surface are  $\sigma_{nn} = \mathbf{n} \cdot \boldsymbol{\sigma} \cdot \mathbf{n}$  and  $\sigma_{n\perp} = \mathbf{n} \times (\boldsymbol{\sigma} \cdot \mathbf{n}) \times \mathbf{n}$ , respectively. We note that the jump conditions are represented in a form which readily allows for physical interpretation.

The jump condition (3.50) states that the mass flux is continuous across the flame. Though our analysis covers only a first perturbative correction of the jump conditions for thin flames, we claim that it is possible to define the flame surface position such that the normal mass flux is continuous at the flame surface to any accuracy desired. Note that the flame surface position used in the analysis does not coincide with the maximum reaction rate. In the reaction sheet approximation it is shown that the surface position is an isotherm of the reactive model, where the temperature is approximately  $T^* = 1 + 0.2(T_b - 1)$ .



The normal momentum flux is discontinuous across the flame according to (3.51). The jump is proportional to the curvature of the flame. Relation (3.51) shows an analogy to the corresponding relation for a fluid interface separating two immiscible fluids:

$$[p - \sigma_{nn}] = 2c\sigma_s, \quad (3.55)$$

where  $\sigma_s > 0$  represents the surface tension of the interface. If we allow for mass transfer  $m$  across the surface, for example by evaporation, then a term  $[mv_n]$  must be added to the left-hand side, so that

$$[mv_n + p - \sigma_{nn}] = 2c\sigma_s. \quad (3.56)$$

Comparing (3.51) to (3.56) we see that the term  $-Pe^{-1}mI_\sigma$  in our problem, with  $I_\sigma$  defined in (3.49), is the analogue of surface tension in the immiscible fluid problem. As discussed above, the integral  $I_\sigma$  is positive so that the ‘surface tension’ of the flame is negative. We therefore refer to it as *surface compression*. This distinguishes the term from conventional surface tension. Also, the term *surface compression* accounts for the fact that it arises due to compressibility effects. In particular, surface compression results from variable density in the stress tensor, and from dynamic pressure changes due to acceleration as the density decreases. With increasing thermal expansion the surface compression rapidly grows in absolute value. Clearly, surface compression has strong implications for the stability of a flame. While surface tension stabilizes fluid interfaces, i.e. it requires energy to increase the area of a fluid interface, we expect that surface compression destabilizes the flame. This effect will be significant if the surface compression is large, i.e. for large thermal expansion. However, the stability of a flame also depends on the flame speed relation, which is the subject of the next section.

From (3.52) we conclude that the tangential momentum (3.52) is in general not continuous across the flame. There are tangential forces, which are proportional to the tangential derivative of surface compression. The derivative of the surface compression is analogous to Marangoni forces which are observed if surface tension is non-uniform along a fluid interface. However, it should be noted that for near-equidiffusional flames, as considered in Matalon & Matkowsky (1982), the flame structure is to leading order constant along the flame, so that this effect is negligibly small.

All the results obtained in the previous sections are valid for arbitrary chemistry and arbitrary dependence of the transport coefficients on the temperature. Therefore, the results are applicable for complex chemical kinetics as well.

#### 4. Asymptotic derivation of the flame speed relation

In the previous sections we discussed the flow. We now determine the flame speed relation. We consider a first-order ( $n = 1$ ) single-step Arrhenius reaction



with high activation energy. The reaction is limited by a single deficient reactant of normalized concentration  $Y$ , so that  $Y$  is unity in the fresh mixture and zero in the burned mixture since it has been completely consumed. Similarly, the normalized temperature in the fresh mixture is unity and the normalized adiabatic combustion temperature is  $T_b$  which is attained in the burned mixture behind the flame. The activation energy of the reaction is assumed to be large, i.e. the Zeldovich number

$Ze$  is assumed to be large, so that the reaction zone is thin. At temperatures lower than  $T_b - O(1/Ze)$  the reaction rate is exponentially small. Within the reaction zone complete conversion is attained, since the reaction rate is appreciable at temperatures close to the adiabatic combustion temperature  $T_b$ . In the limit  $Ze \rightarrow \infty$  the reaction zone shrinks to a surface. Analysis of the reaction zone (Matkowsky & Sivashinsky 1979) allows us to rewrite the reaction term in terms of the Dirac delta function  $\delta$  as

$$W = Pe W_r \delta(X - X_r), \quad W_r = \exp(Ze(T_r - T_b)(T_b - 1)^{-1}), \quad (4.2)$$

where  $X_r$  is the position of the reaction surface in our moving system of coordinates whose origin does not coincide with the reaction zone, and  $T_r$  is the temperature at the reaction surface. In terms of the reduced enthalpy  $H$ , the strength of the delta function in the reaction term becomes

$$W_r = \exp(Ze(1 - Le^{-1})H_r), \quad (4.3)$$

where  $H_r$  is  $H$  evaluated at the reaction zone. It should be noted that the analysis of the reaction zone (Matkowsky & Sivashinsky 1979) was carried out only for  $Le$  near 1, though it was also employed in Sivashinsky (1976). The result is also valid for near-planar flames for arbitrary  $Le$ . In this paper we consider  $O(1)$  flame curvature on the hydrodynamic length scale, so that the radius of curvature viewed on the flame structure length scale is  $O(Pe)$ , i.e. we effectively consider nearly planar flames, so that the result is valid here as well.

The flame speed relation is derived from the conservation equations for the reduced enthalpy  $H$  and the fuel concentration  $Y$ . Due to the scaling of  $H$  the enthalpy is  $O(1)$  for any  $Le$ , so that it is not necessary to consider the case  $Le \approx 1$  separately. We recall that the reduced enthalpy replaces the temperature equation. However, since in previous theories the temperature and enthalpy were considered, rather than concentration and enthalpy, we will still solve for the leading-order temperature and express the results in terms of the temperature, even though the temperature could be omitted.

To derive the desired flame speed relation we first solve the leading-order temperature, concentration and enthalpy equations, employing the intrinsic disturbed flame equation (3.5) and the corresponding fluxes (2.17)–(2.19). The leading-order solutions are substituted into the intrinsic disturbed flame jump conditions (3.7) and (3.8) to yield the enthalpy at the discontinuity surface and the propagation speed of the discontinuity surface.

Integrating the leading-order intrinsic disturbed flame equation (3.5) for the concentration, temperature, and enthalpy from  $X = -\infty$  to arbitrary  $X$  we obtain

$$J_{(0)}^1(RY) - m_{(0)} = -W_{r(0)}U(X - X_r), \quad (4.4)$$

$$J_{(0)}^1(RT) - m_{(0)} = (T_b - 1)W_{r(0)}U(X - X_r), \quad (4.5)$$

$$J_{(0)}^1(RH) = 0, \quad (4.6)$$

where  $U$  denotes the Heaviside unit step function and  $m_{(0)}$  represents the contribution from the left-hand boundary ( $X \rightarrow -\infty$ ) where  $Y_{(0)} = T_{(0)} = 1$  and  $H_{(0)} = 0$ . The fluxes are

$$J_{(0)}^1(RY) = m_{(0)}Y_{(0)} - Le^{-1}\Lambda\partial Y_{(0)}/\partial X, \quad (4.7)$$

$$J_{(0)}^1(RT) = m_{(0)}T_{(0)} - \Lambda\partial T_{(0)}/\partial X, \quad (4.8)$$

$$J_{(0)}^1(RH) = m_{(0)}H_{(0)} - \Lambda(\partial(H_{(0)} + Y_{(0)})/\partial X). \quad (4.9)$$

Ahead of the reaction surface the right-hand side vanishes and we thus obtain homogeneous first-order ordinary differential equations to determine the concentration, temperature, and enthalpy as functions of  $X$ . The mass flux  $m_{(0)}$  is still undetermined. The leading-order solutions are

$$Y_{(0)} = 1 - \exp(Le m_{(0)}(\zeta - \zeta_r)), \quad \zeta = \int_0^X \frac{1}{\Lambda} dX, \quad (4.10)$$

$$\Theta = (T_{(0)} - 1)(T_b - 1)^{-1} = \exp(m_{(0)}(\zeta - \zeta_r)). \quad (4.11)$$

The concentration may be expressed in terms of the temperature as  $Y_{(0)} = 1 - \Theta^{Le}$ . Similarly, the reduced enthalpy may be written as

$$H_{(0)} = (1 - Le^{-1})^{-1}(\Theta - \Theta^{Le}). \quad (4.12)$$

Note that  $H_{(0)} > 0$  for any Lewis number. Behind the reaction surface  $T_{(0)} = T_b$  and  $Y_{(0)} = H_{(0)} = 0$ . Behind the reaction surface the hydrodynamic model enthalpy  $h$  is identical to the reactive model enthalpy  $H$  so that we conclude that  $h_{(0)} = 0$  everywhere.

Applying the intrinsic disturbed flame jump condition (3.7) for the concentration yields

$$m_{(0)} = W_{r(0)}, \quad (4.13)$$

where we used  $[J_{(0)}^1(\rho y)] = -m_{(0)}$  and  $\int_{-\infty}^{\infty} Q_{(0)}(RY) dX = -W_{r(0)}$ . The corresponding jump condition for the enthalpy shows that indeed

$$h_{r(0)} = H_{r(0)} = 0. \quad (4.14)$$

At  $O(Pe^{-1})$  it is sufficient to analyse the intrinsic disturbed flame jump conditions (3.8) for concentration and enthalpy since we are not interested in the actual solutions of the reactive model. Note that the tangential fluxes  $J_{(0)}^\alpha(RY)$ ,  $J_{(0)}^\alpha(RT)$ , and  $J_{(0)}^\alpha(RH)$  vanish at leading order, due to the specific choice of our coordinate system so that the second integral in (3.8) vanishes:

$$\begin{aligned} \left(\frac{\partial}{\partial t} + \chi^*\right) \int_{-\infty}^{\infty} (R_{(0)}Y_{(0)} - \rho_{(0)}y_{(0)}) dX - m_{(1)} \\ = \int_{-\infty}^{\infty} (Q_{(1)}(RY) - 2cX Q_{(0)}(RY)) dX, \end{aligned} \quad (4.15)$$

$$\left(\frac{\partial}{\partial t} + \chi^*\right) \int_{-\infty}^{\infty} (R_{(0)}H_{(0)} - \rho_{(0)}h_{(0)}) dX + [J_{(1)}^1(\rho h)] = 0, \quad (4.16)$$

where  $\int_{-\infty}^{\infty} (Q_{(1)}(RY) - 2cX Q_{(0)}(RY)) dX = -(W_{r(1)} - 2cX_r W_{r(0)})$ ,  $h_{(0)} = 0$  for any  $X$ , and  $\rho_{(0)}y_{(0)} = 1$  for  $X < 0$  and  $\rho_{(0)}y_{(0)} = 0$  otherwise. Thus, we obtain

$$\left(\frac{\partial}{\partial t} + \chi^*\right) \left( \int_{-\infty}^{X_r} (1 - R_{(0)}Y_{(0)}) dX - \int_0^{X_r} dX \right) + m_{(1)} = W_{r(1)} - 2cX_r m_{(0)}, \quad (4.17)$$

$$\left(\frac{\partial}{\partial t} + \chi^*\right) \int_{-\infty}^{X_r} R_{(0)}H_{(0)} dX + [J_{(1)}^1(\rho h)] = 0. \quad (4.18)$$

The jump  $[J_{(1)}^1(\rho h)] = m_{(0)}h_{b(1)}^*$ , where  $h_{b(1)}^* = H_{r(1)}$  since gradients of  $h$  are  $O(Pe^{-2})$  in the burned region and since the enthalpies of the hydrodynamic and the reactive

models are identical behind the reaction surface. After introducing the integrals

$$I_Y = m_{(0)} \int_{-\infty}^{X_r} (1 - R_{(0)} Y_{(0)}) dX = m_{(0)} \int_{-\infty}^{X_r} R_{(0)} (1 - Y_{(0)}) dX + m_{(0)} \int_{-\infty}^{X_r} (1 - R_{(0)}) dX,$$

$$I_H = m_{(0)} \int_{-\infty}^{X_r} R_{(0)} H_{(0)} dX,$$

$$I_X = m_{(0)} X_r = m_{(0)} \int_{-\infty}^{X_r} dX,$$

which will be shown to be constants, we obtain

$$m_{(1)} + (I_Y - I_X)(\partial/\partial t + \chi)(1/m_{(0)}) + 2cI_X = W_{r(1)}, \quad (4.19)$$

$$m_{(0)} h_{b(1)}^* + I_H(\partial/\partial t + \chi)(1/m_{(0)}) = 0, \quad (4.20)$$

which together with (4.3),  $h_{b(1)}^* = H_{r(1)}$ , and the leading-order solutions (4.13) and (4.14), determine the mass flux and the enthalpy at the flame.

The quantity  $X_r = I_X/m_{(0)}$  is the distance between the discontinuity surface and the reaction surface, which in general is not constant. Since the density integral  $I_R$  defined in (3.41) vanishes,  $I_X = I_X - I_R m_{(0)} T_b/(T_b - 1)$ . Now the integrals have the same kernel in the fresh and the burned mixtures and we obtain

$$I_X = m_{(0)} T_b/(T_b - 1) \int_{-\infty}^{X_r} (1 - 1/T) dX.$$

To determine  $X_r$  we employ (3.47) to convert the integral into one with respect to temperature. Similarly, we express the integrals  $I_Y$  and  $I_H$  in terms of the temperature  $\Theta$  using  $dX = \Lambda_{(0)}/(\Theta m_{(0)}) d\Theta$ ,  $R_{(0)} = T_{(0)}^{-1} = ((T_b - 1)\Theta + 1)^{-1}$ , and  $\Lambda_{(0)} = T_{(0)}^{1/2} = ((T_b - 1)\Theta + 1)^{1/2}$ . This yields

$$I_Y = \int_0^1 ((T_b - 1)\Theta + 1)^{-1/2} \Theta^{Le-1} d\Theta + 2(T_b^{1/2} - 1), \quad (4.21)$$

$$I_H = \frac{1}{1 - Le^{-1}} \int_0^1 ((T_b - 1)\Theta + 1)^{-1/2} (1 - \Theta^{Le-1}) d\Theta, \quad (4.22)$$

$$I_X = 2T_b(T_b^{1/2} + 1)^{-1}. \quad (4.23)$$

Note that the integrals  $I_Y$ ,  $I_H$  and  $I_X$  are independent of the mass flux  $m_{(0)}$ .

Let us briefly discuss the behaviour of the integrals  $I_Y$ ,  $I_H$  and  $I_X$ . The integral  $I_Y$  is positive. Typically, the second term  $2(T_b^{1/2} - 1)$  is dominant; typical values for the first term are between 0.2 for large Lewis numbers and 2 for small Lewis numbers.

The integral  $I_H > 0$  only weakly depends on the parameters. Its value decreases with increasing Lewis numbers and reaches an asymptote as  $Le \rightarrow \infty$ . For  $T_b \rightarrow 1$  the integral  $I_H \rightarrow 1$  and  $I_H$  decreases with growing  $T_b$ . Typical values of  $I_H$  are approximately 0.7.

The integral  $I_X > 0$  grows with thermal expansion. For typical combustion conditions  $I_X \approx 3$ .

Since the form of the flame speed relation will change depending on the relative sizes of the parameters  $Pe$ ,  $Ze$ , and  $(Le^{-1} - 1)$ , we first write the relations in terms of

these parameters, retaining both the  $O(1)$  and the  $O(Pe^{-1})$  terms. We thus have

$$m + Pe^{-1}((I_Y - I_X)(\partial/\partial t + \chi)(1/m) + 2cI_X) = \exp(Ze(1 - Le^{-1})h_b^*) + o(Pe^{-1}), \quad (4.24)$$

$$mh_b^* + Pe^{-1}I_H(\partial/\partial t + \chi)(1/m) = 0 + o(Pe^{-1}). \quad (4.25)$$

The time derivative in (4.24) may be neglected, as the  $Pe^{-1}$  term is relevant only for near-equidiffusional flames where  $m \approx 1 + O(Pe^{-1})$ , so that the time derivative term is  $O(Pe^{-2})$ . Eliminating  $h_b^*$ , the hydrodynamic model enthalpy in the burned region behind the discontinuity surface, results in the general flame speed relation

$$CI_H(\partial/\partial t + \chi)(1/m) + m \ln(m + Pe^{-1}((I_Y - I_X)\chi/m + 2cI_X)) = 0, \quad (4.26)$$

where

$$C = Pe^{-1}Ze(1 - Le^{-1}) \quad (4.27)$$

is a non-dimensional number which accounts for the combined effects of the Lewis, Péclet and Zeldovich numbers. Note that  $Le > 1$  corresponds to  $C > 0$ . The parameter  $C$  depends on  $Le$  and  $Ze$ , which are associated with the flame, and on  $Pe$ , which is associated with the fluid flow. It may be interpreted as the ratio of the transverse length scale of the flame to the hydrodynamic length scale, and is related to the Markstein number. Alternatively,  $C$  may be interpreted as the ratio of the response time of the flame to hydrodynamic disturbances to the hydrodynamic time  $\tilde{l}/\tilde{s}_F^0$ .

The various limits discussed in the literature can easily be obtained from (4.26).

#### 4.1. The effect of short wavelengths

Before discussing the flame speed relation for various parameter regimes, we first modify the relation. We recall that in deriving the flame speed relation we only considered variations with  $O(1)$  wavelength, tacitly neglecting short-wave variations. We now include the effect of short waves, which will be important for stability considerations.

In order to analyse the effect of short waves we must redo the analysis with modified scalings. We first define appropriate scalings, then derive modified intrinsic disturbed flame equations, next discuss the jump conditions and finally derive a modified flame speed relation.

We assume that the short-wavelength flame wrinkles are very small in amplitude, thus effectively assuming that the flame curvature is small. We wish to determine their effect on the flame speed relation (4.26). The length scale of short-wave perturbations is  $o(1)$ . A distinguished limit corresponds to perturbations whose transverse length scale is  $O(Pe^{-1/2})$ . We introduce the stretched transverse variables  $\xi^\alpha = Pe^{1/2}x^\alpha$ , so that derivatives with respect to  $\xi^\alpha$  are  $O(1)$ .

As the problem now involves fractional powers of the Péclet number we expand the dependent variables in powers of  $Pe^{-1/2}$ , i.e.  $F \sim F_{(0)} + Pe^{-1/2}F_{(1/2)} + Pe^{-1}F_{(1)} + \dots$ , where  $F$  denotes any of the variables which are expanded. We still expand the quantities associated with the coordinate system  $\sqrt{g}$ ,  $g^{ij}$  into Taylor series in powers of  $Pe^{-1}$ . This might seem to represent a contradiction, as short-wave changes along the flame should also induce normal variations of the coordinate system on a short length scale. However, this is only the case if the amplitude of the short-wave wrinkles of the flame is  $O(1)$ . If we expanded  $\sqrt{g}$ ,  $g^{ij}$  in powers of  $Pe^{-1/2}$  as well, we would recover the previous analysis exactly, where now all the previous results would appear at  $O(Pe^{-1/2})$ . Now that we have assumed that the outer flow varies on an  $O(Pe)$

length scale, we may ask how it is possible that we observe  $O(Pe^{1/2})$  variations along the flame. They are due to variations of the direction of the normal vector in the presence of short-wave wrinkles. To illustrate, consider a uniform outer flow and an initially flat flame. Now consider short-wave wrinkles along the flame without modifying the outer flow. Since the flame is no longer flat, the normal direction on the flame is no longer eqnarrayed with the flow direction. The local tangential and normal components of the flow depend on the direction of the normal vector so that we observe variations in the components on the length scale of the wrinkles, even though the outer flow does not exhibit any variations.

Having defined the appropriate scalings we now modify the intrinsic disturbed flame equations. Employing the new scalings, the intrinsic disturbed flame equations become

$$\frac{\partial}{\partial X} (J_{(0)}^1(\Phi)) = Q_{(0)}(\Phi), \quad (4.28)$$

$$\frac{1}{\sqrt{g^*}} \frac{\partial}{\partial \xi^\alpha} (\sqrt{g^*} J_{(0)}^\alpha(\Phi)) + \frac{\partial}{\partial X} (J_{(1/2)}^1(\Phi)) = Q_{(1/2)}(\Phi), \quad (4.29)$$

$$\begin{aligned} \left( \frac{\partial}{\partial t} + \chi \right) \Phi_{(0)} + \frac{1}{\sqrt{g^*}} \frac{\partial}{\partial \xi^\alpha} (\sqrt{g^*} J_{(1/2)}^\alpha(\Phi)) + \frac{\partial}{\partial X} (J_{(1)}^1(\Phi) - 2cX J_{(0)}^1(\Phi)) \\ = Q_{(1)}(\Phi) - 2cX Q_{(0)}(\Phi). \end{aligned} \quad (4.30)$$

Similarly, we write three terms of the intrinsic disturbed flame jump conditions

$$[J_{(0)}^1(\phi)] = \int_{-\infty}^{\infty} Q_{(0)}(\Phi) dX, \quad (4.31)$$

$$\int_{-\infty}^{\infty} \frac{1}{\sqrt{g^*}} \frac{\partial}{\partial x^\alpha} (\sqrt{g^*} (J_{(0)}^\alpha(\Phi) - J_{(0)}^\alpha(\phi))) dX + [J_{(1/2)}^1(\phi)] = \int_{-\infty}^{\infty} Q_{(1/2)}(\Phi) dX, \quad (4.32)$$

$$\begin{aligned} [J_{(1)}^1(\phi)] = \int_{-\infty}^{\infty} (Q_{(1)}(\Phi) - 2cX Q_{(0)}(\Phi)) dX - \left( \frac{\partial}{\partial t} + \chi^* \right) \int_{-\infty}^{\infty} (\Phi_{(0)} - \phi_{(0)}) dX \\ - \int_{-\infty}^{\infty} \frac{1}{\sqrt{g^*}} \frac{\partial}{\partial x^\alpha} (\sqrt{g^*} (J_{(1/2)}^\alpha(\Phi) - J_{(1/2)}^\alpha(\phi))) dX. \end{aligned} \quad (4.33)$$

When we consider short-wave perturbations of the flame the equations and jump conditions (4.28)–(4.33) replace (3.5)–(3.8).

Employing the modified intrinsic disturbed flame equations we next discuss the effect of short waves on the flow. Since the flame thickness is  $O(Pe^{-1})$ , i.e. variations across the flame are much stronger than variations along the flame, the analysis of the leading-order equations remains unchanged. Comparing the intrinsic disturbed flame jump conditions (4.32) for short waves to (3.8) for  $O(1)$  waves, we observe that the equations for the  $O(Pe^{-1/2})$  quantities are similar to the equations for  $O(Pe^{-1})$  quantities. However the  $(\partial/\partial t + \chi)$  operator and the curvature  $c$  do not yet appear. Thus, solutions of the flow equations at  $O(Pe^{-1/2})$  are identical to the previous  $O(Pe^{-1})$  solutions if we drop the terms multiplying  $(\partial/\partial t + \chi)$  and  $c$ .

The continuity equation now implies that the normal mass flux  $M_{(1/2)}^1 = m_{(1/2)}^1 = m_{(1/2)}$  is constant across the flame. Note that at  $O(Pe^{-1/2})$  there is no need to specify the precise location of the discontinuity surface. In the momentum

jump condition (3.40) the curvature term no longer appears so that it simplifies to

$$[m_{(0)}v_{(1/2)}^i + m_{(1/2)}v_{(0)}^i + g^{i*}p_{(1/2)} - \sigma_{(1/2)}^{i1}]l_i^* = -\left(g^{\alpha\beta*}l_\beta^* \frac{\partial}{\partial \xi^\alpha}\right)m_{(0)}I_\sigma, \quad (4.34)$$

which is easily decomposed into normal and tangential jump conditions. Since curvature is too weak, there are no normal forces due to surface compression at  $O(Pe^{-1/2})$ . However, there are tangential forces along the flame, due to the rapid change in surface compression. Thus, here the Marangoni effect dominates surface compression. Combining the leading-order and  $O(Pe^{-1/2})$  terms of the fluid jump conditions yields

$$[mv^1 + p] = o(Pe^{-1/2}), \quad [mv^\alpha] = -Pe^{-1}g^{\alpha\beta*} \frac{\partial}{\partial x^\beta}(mI_\sigma) + o(Pe^{-1/2})$$

so that we do not find any terms that were not already present in (3.50)–(3.52). Note that the additional terms in (3.50)–(3.52) are negligible for the case of short-wave perturbations. Thus, the fluid jump conditions (3.50)–(3.52) are applicable for both  $O(1)$  and short-wave wrinkles of the flame front.

Before considering the first three terms of the enthalpy and concentration equations to derive the flame speed equation, we must discuss the tangential mass flux, which enters the equations. The Marangoni effect results in a jump of the tangential flow  $[v_{(1/2)}^\alpha]$  so that  $v_{(1/2)}^\alpha \neq V_{(1/2)}^\alpha$  in the flame zone. As the tangential flow changes within the flame structure, the tangential mass flux  $M_{(1/2)}^\alpha = R_{(0)}(V_{(1/2)}^\alpha - u_{(1/2)}^{\alpha*})$  becomes non-constant as well at  $O(Pe^{-1/2})$ . Here,  $u_{(1/2)}^{\alpha*}$  is the tangential speed of the coordinate system, which is constant across the flame structure. At the leading order we choose the tangential speed of the coordinate system such that the tangential mass flux vanishes. At  $O(Pe^{-1/2})$ , the tangential flow speed changes along the normal direction while the speed of the coordinate system is constant in this direction. Thus,  $M_{(1/2)}^\alpha$  cannot be made to vanish at all points along the normal direction. However, we are free to choose  $u_{(1/2)}^{\alpha*}$  at our convenience. Below, it will be chosen to make a certain term (cf. (4.39)) vanish.

The final step is to derive the flame speed equation. We are interested, in particular, in the case where variations of the flame speed are  $O(1)$  along the flame, i.e.  $C = O(1)$ . In this limit the problem is governed by the leading-order equations for the fluid flow and the concentration and by the enthalpy equation including a perturbative correction. Therefore, it is sufficient to consider the enthalpy equation. Perturbative corrections in the other equations are important only when the new terms that we derive below are negligibly small. However, perturbative corrections of the flow variables enter the enthalpy equation through the transverse flux term and thus are considered. We will not discuss all the details of the analysis since most of the steps are identical to the previous analysis. Rather, we discuss the key steps and point out the differences.

The fluxes in the enthalpy equation become

$$J_{(0)}^1(RH) = m_{(0)}H_{(0)} - \Lambda \frac{\partial}{\partial X}(H_{(0)} - Y_{(0)}), \quad J_{(0)}^\alpha(RH) = 0, \quad (4.35)$$

$$J_{(1/2)}^1(RH) = m_{(1/2)}H_{(0)} + m_{(0)}H_{(1/2)} - \Lambda \frac{\partial}{\partial X}(H_{(1/2)} - Y_{(1/2)}), \quad (4.36)$$

$$J_{(1/2)}^\alpha(RH) = M_{(1/2)}^\alpha H_{(0)} - \Lambda g^{\alpha\beta} \frac{\partial}{\partial \xi^\beta}(H_{(0)} - Y_{(0)}), \quad (4.37)$$

$$J_{(1)}^1(RH) = M_{(1)}^1 H_{(0)} + m_{(1/2)}H_{(1/2)} + m_{(0)}H_{(1)} - \Lambda \frac{\partial}{\partial X}(H_{(1)} - Y_{(1)}). \quad (4.38)$$

From (4.29) we conclude that  $J_{(1/2)}^1(RH)=0$  and that the enthalpy  $H_{(1/2)}$  vanishes within the flame structure, and at the reaction surface in particular. The mass flux  $m_{(0)}$  is as yet undetermined.

At  $O(Pe^{-1})$  the intrinsic disturbed flame jump condition (4.33) becomes

$$\left(\frac{\partial}{\partial t} + \chi\right) \int_{-\infty}^{X_r} R_{(0)} H_{(0)} dX + \frac{1}{\sqrt{g^*}} \int_{-\infty}^{X_r} \frac{\partial}{\partial \xi^\alpha} (\sqrt{g^*} J_{(1/2)}^\alpha(RH)) dX + m_{(0)} h_{b(1)}^* = 0. \quad (4.39)$$

where we have employed the fact that the hydrodynamic model's contributions to the integrals vanish. The flux  $J_{(1/2)}^\alpha(RH)$  which appears in (4.38), is defined in (4.36) and involves  $M_{(1/2)}^\alpha$ , which is as yet undetermined. However, it is not necessary to calculate  $M_{(1/2)}^\alpha$  if we choose  $u_{(1/2)}^{\alpha*}$  such that

$$\int_{-\infty}^{X_r} \frac{\partial}{\partial \xi^\alpha} (\sqrt{g^*} M_{(1/2)}^\alpha H_{(0)}) dX = 0, \quad (4.40)$$

which can be done without loss of generality. The integral (4.39) is part of the term  $\int_{-\infty}^{X_r} (\partial(g^{1/2*} J_{(1/2)}^\alpha(RH))/\partial \xi^\alpha) dX$  in (4.38) and is the only term which involves  $M_{(1/2)}^\alpha$ . This term now vanishes. For our analysis it is not necessary to calculate the value of  $u_{(1/2)}^{\alpha*}$  since we are not interested in calculating perturbative corrections to the flame stretch. Note that our definition  $u_{(0)}^{\alpha*} = v_{(0)}^{\alpha*}$  at leading order may also be written in a form similar to (4.39). The tangential speed  $u^{\alpha*}$  of the coordinate system at the discontinuity surface, and thus the flame stretch, is now defined by an enthalpy integral. This approach may even be applied to define the flame stretch of thick flames.

Consider the transverse derivative term in (4.38) which was not present in the analyses of Matalon & Matkowsky (1982), Sivashinsky (1976) and Klimenko & Class (2000):

$$\begin{aligned} & \int_{-\infty}^{X_r} \frac{\partial}{\partial \xi^\alpha} (\sqrt{g^*} J_{(1/2)}^\alpha(RH)) dX \\ &= \int_{-\infty}^{X_r} \frac{\partial}{\partial \xi^\alpha} \left( \sqrt{g^*} M_{(1/2)}^\alpha H_{(0)} - \sqrt{g^*} g_{(0)}^{\alpha\beta*} \Lambda_{(0)} \frac{\partial}{\partial \xi^\beta} (H_{(0)} - Y_{(0)}) \right) dX + o(1), \end{aligned} \quad (4.41)$$

where the term involving  $M_{(1/2)}^\alpha$  vanishes due to (4.39). We note that  $H_{(0)} - Y_{(0)}$  can be expressed in terms of the temperature or  $\Theta = (T - 1)/(T_b - 1)$ , i.e.

$$\frac{\partial}{\partial \xi^\beta} (H_{(0)} - Y_{(0)}) = \left( \frac{\partial}{\partial \Theta} (H_{(0)} - Y_{(0)}) \right) \frac{\partial \Theta}{\partial \xi^\beta}, \quad (4.42)$$

where

$$\frac{\partial}{\partial \Theta} (H_{(0)} - Y_{(0)}) = \frac{1 - \Theta^{Le-1}}{1 - Le^{-1}}. \quad (4.43)$$

For convenience, we henceforth drop the index (0) in  $m_{(0)}$ ,  $\Lambda_{(0)}$ ,  $H_{(0)}$ ,  $Y_{(0)}$  and  $g_{(0)}^{\alpha\beta*}$ . The derivative  $\partial\Theta/\partial\xi^\beta$  is calculated from  $\Theta = \exp(m(\zeta - \zeta_r))$ , where  $m$  is a function of  $\xi^\beta$ . Finally,  $\partial\Theta/\partial\xi^\beta = (\partial\Theta/\partial(1/m))(\partial(1/m)/\partial\xi^\beta)$  where  $\partial\Theta/\partial(1/m) = \Theta \ln(1/\Theta)m$ .

Similarly,

$$\begin{aligned} & \frac{\partial}{\partial \xi^\alpha} \sqrt{g^*} g^{\alpha\beta*} \Lambda \frac{\partial}{\partial \xi^\beta} (H - Y) \\ &= \frac{\partial}{\partial \xi^\alpha} \left( \Lambda \frac{1 - \Theta^{Le-1}}{1 - Le^{-1}} \Theta \ln(1/\Theta) m \sqrt{g^*} g^{\alpha\beta*} \frac{\partial(1/m)}{\partial \xi^\beta} \right) \end{aligned}$$



$$\begin{aligned}
 &= \frac{\partial}{\partial \Theta} \left( \Lambda \frac{1 - \Theta^{Le-1}}{1 - Le^{-1}} \Theta \ln(1/\Theta) \right) \Theta \ln(1/\Theta) m \left( m \sqrt{g^*} g^{\alpha\beta*} \frac{\partial(1/m)}{\partial \xi^\alpha} \frac{\partial(1/m)}{\partial \xi^\beta} \right) \\
 &\quad + \Lambda \frac{1 - \Theta^{Le-1}}{1 - Le^{-1}} \Theta \ln(1/\Theta) m \left( \frac{1}{m} \frac{\partial}{\partial \xi^\alpha} \left( m \sqrt{g^*} g^{\alpha\beta*} \frac{\partial(1/m)}{\partial \xi^\beta} \right) \right) \\
 &= \left( \frac{\partial}{\partial \Theta} \left( \Lambda \frac{1 - \Theta^{Le-1}}{1 - Le^{-1}} \Theta \ln(1/\Theta) \right) - \Lambda \frac{1 - \Theta^{Le-1}}{1 - Le^{-1}} \right) \Theta \ln(1/\Theta) m \\
 &\quad \times \left( m \sqrt{g^*} g^{\alpha\beta*} \frac{\partial(1/m)}{\partial \xi^\alpha} \frac{\partial(1/m)}{\partial \xi^\beta} \right) + \Lambda \frac{1 - \Theta^{Le-1}}{1 - Le^{-1}} \Theta \ln(1/\Theta) m \\
 &\quad \times \left( \frac{\partial}{\partial \xi^\alpha} \left( \sqrt{g^*} g^{\alpha\beta*} \frac{\partial(1/m)}{\partial \xi^\beta} \right) \right), \tag{4.44}
 \end{aligned}$$

so that

$$\begin{aligned}
 &\int_{-\infty}^{X_r} \frac{\partial}{\partial \xi^\alpha} \sqrt{g^*} g^{\alpha\beta*} \Lambda \frac{\partial}{\partial \xi^\beta} (H - Y) dX \\
 &\quad = I_\Delta \frac{\partial}{\partial \xi^\alpha} \left( \sqrt{g^*} g^{\alpha\beta*} \frac{\partial(1/m)}{\partial \xi^\beta} \right) - I_{\nabla^2} \left( m \sqrt{g^*} g^{\alpha\beta*} \frac{\partial(1/m)}{\partial \xi^\alpha} \frac{\partial(1/m)}{\partial \xi^\beta} \right). \tag{4.45}
 \end{aligned}$$

The quantities  $I_\Delta$  and  $I_{\nabla^2}$  denote the integrals

$$I_\Delta = \int_{-\infty}^{X_r} \Lambda \ln(1/\Theta) \frac{1 - \Theta^{Le-1}}{1 - Le^{-1}} \Theta m dX, \tag{4.46}$$

$$I_{\nabla^2} = I_\Delta - \int_{-\infty}^{X_r} \ln(1/\Theta) \frac{\partial}{\partial \Theta} \left( \Lambda \frac{1 - \Theta^{Le-1}}{1 - Le^{-1}} \Theta \ln \Theta \right) \Theta m dX. \tag{4.47}$$

Now, replacing integration with respect to  $X$  by integration with respect to  $\Theta$  using  $dX = \Lambda/(\Theta m) d\Theta$  and  $\Lambda = T^{1/2} = ((T_b - 1)\Theta + 1)^{1/2}$  yields

$$\begin{aligned}
 I_\Delta &= \int_0^1 \Lambda^2 \ln(1/\Theta) \frac{1 - \Theta^{Le-1}}{1 - Le^{-1}} d\Theta \\
 &= 1 + Le^{-1} + (T_b - 1) Le (3 + Le) / (4(1 + Le)^2), \tag{4.48}
 \end{aligned}$$

$$\begin{aligned}
 I_{\nabla^2} &= I_\Delta - \int_0^1 \Lambda \ln(1/\Theta) \frac{\partial}{\partial \Theta} \left( \Lambda \frac{1 - \Theta^{Le-1}}{1 - Le^{-1}} \Theta \ln(1/\Theta) \right) d\Theta \\
 &= (T_b - 1) (7 + Le (4 + Le)) Le / (8(1 + Le)^3). \tag{4.49}
 \end{aligned}$$

The integrals  $I_\Delta$  and  $I_{\nabla^2}$  are positive constants, independent of  $m$ .

Collecting all  $O(Pe^{-1})$  terms of the intrinsic disturbed flame jump condition (4.33) for the enthalpy finally yields

$$\begin{aligned}
 I_H (\partial/\partial t + \chi) (1/m) - I_\Delta \frac{1}{\sqrt{g^*}} \frac{\partial}{\partial \xi^\alpha} \left( \sqrt{g^*} g^{\alpha\beta*} \frac{\partial(1/m)}{\partial \xi^\beta} \right) \\
 + I_{\nabla^2} \left( m g^{\alpha\beta*} \frac{\partial(1/m)}{\partial \xi^\alpha} \frac{\partial(1/m)}{\partial \xi^\beta} \right) + m h_{b(1)}^* = 0. \tag{4.50}
 \end{aligned}$$

Note that  $h_{b(1)}^*$  is the jump of the enthalpy across the discontinuity surface. In coordinate-invariant form  $g^{-1/2*} \partial(g^{1/2*} g^{\alpha\beta*} (\partial(1/m)/\partial \xi^\beta)) / \partial \xi^\alpha$  becomes

$$Pe^{-1} \nabla_\perp^2 (1/m) = Pe^{-1} \nabla \cdot (\mathbf{n} \times \nabla(1/m) \times \mathbf{n}) \tag{4.51}$$

and  $mg^{\alpha\beta*}(\partial(1/m)/\partial\xi^\alpha)(\partial(1/m)/\partial\xi^\beta)$  becomes

$$Pe^{-1}m(\nabla_\perp(1/m))^2 = Pe^{-1}m(\mathbf{n} \times \nabla(1/m) \times \mathbf{n}) \cdot (\mathbf{n} \times \nabla(1/m) \times \mathbf{n}). \quad (4.52)$$

The operator  $\nabla_\perp^2$  is the surface Laplacian. Neighbouring points on the flame cannot propagate at arbitrary speeds. The spatial coupling of neighbouring flame elements is ensured by the diffusive nature of  $\nabla_\perp^2$ , which prohibits the development of very short-wavelength wrinkles along the flame. The second new term is nonlinear and provides a second mechanism for the coupling of neighbouring flame elements. It is more pronounced for large flame speed gradients along the flame. Now, the flame speed relation becomes the partial differential equation

$$C(I_H(\partial/\partial t + \chi)(1/m) - Pe^{-1}I_\Delta\nabla_\perp^2(1/m) + Pe^{-1}I_{\nabla^2}m(\nabla_\perp(1/m))^2) + m \ln(m + Pe^{-1}((I_Y - I_X)\chi/m + 2cI_X)) = 0. \quad (4.53)$$

Note that we could derive similar terms for the concentration equation. However, these do not contribute to the final result, as the  $O(Pe^{-1})$  term in the concentration equation is important only for near-equidiffusional flames, where  $m = 1$  at leading order, so that the new term is negligible. The relation (4.52) generalizes the flame speed relation (4.26) to include the effect of short waves. We refer to it as the *unified flame speed relation*. Note that in all previous analyses the transverse coupling terms did not appear, since only  $O(1)$  wavelength perturbations of the flame front were considered. We note that the terms involving  $I_\Delta$  and  $I_{\nabla^2}$  are both stabilizing. We next analyse (4.52) in various parameter ranges. Before doing so, we show that density variations in the burned region are indeed negligible. The order to which each term must be calculated is not immediately apparent, since our model is applicable for a wide parameter range. The necessary accuracy can be determined from the flame speed  $m$ . The relation (4.52) determines the deviation of  $m$  from the adiabatic flame speed 1, i.e.  $m - 1$ , which may be  $O(1)$  or  $o(1)$ . In either case, all other quantities in the model must be calculated to  $O(m - 1)$ . We will show that constant density may be assumed in the burned region, which is the case if  $\rho - \rho_b = o(m - 1)$ . We determine the asymptotic orders of  $m - 1$  and  $\rho - \rho_b$  in terms of the other parameters and compare them. Except for  $Pe$  and  $C$  all the parameters in (4.52) are  $O(1)$ .  $C$  may be either  $O(1)$  or  $o(1)$ . Thus,  $m = O(1)$  if  $C = O(1)$  and  $m = 1 + O(Pe^{-1})$  if  $C = O(Pe^{-1})$ , so in either case  $m - 1 = O(C)$ . In the burned region  $\rho - \rho_b = \rho - 1/T_b$  is of the same order as  $\vartheta - T_b$ , i.e.  $\rho - \rho_b = O((1 - Le^{-1})h)$  where enthalpy  $h$  has been employed rather than temperature. From  $H_{(0)} = H_{(1/2)} = 0$  we conclude that  $h = O(Pe^{-1})$  in the burned region so that  $\rho - \rho_b = O(Pe^{-1}(1 - Le^{-1})) = O(Ze^{-1}C) = o(C)$ . However,  $\rho - \rho_b$  must only be calculated to  $O(m - 1) = O(C)$ , verifying the constant-density assumption employed in the hydrodynamic model, ahead of and behind the flame surface.

#### 4.2. Near-equidiffusional flames: weak flame speed variations ( $C = O(Pe^{-1})$ )

If the Lewis number is close to unity and the Zeldovich number is large, then  $C = Pe^{-1}Ze(1 - Le^{-1}) = O(Pe^{-1})$ , i.e.  $C = Pe^{-1}C_{(1)}$  where  $C_{(1)}$  is  $O(1)$ .

Substituting this into (4.52) and expanding in powers of  $Pe^{-1}$  yields

$$m = 1 - Pe^{-1}(2cI_X + (I_Y + C_{(1)}I_H - I_X)\chi) + o(Pe^{-1}). \quad (4.54)$$

Since  $m$  is unity at leading order the transverse coupling terms become  $O(Pe^{-2})$  and thus are negligibly small. The result is identical to the result of Matalon & Matkowsky, except for the terms multiplying  $I_X$  which originate from the different definitions of the origin of the coordinate system employed in our approach and in

their approach. Recall that for curved flames the normal mass flux  $m_{(1)}^1$  changes along the normal direction, which yields the curvature term. Therefore, the coefficients of curvature and flame stretch in the flame speed relation change with the location of the discontinuity surface. The flame speed relations appearing in previous analyses can be easily compared to our relation, since the definition of the flame position only enters in the integral  $I_X$ , which may be evaluated for any flame position. In particular, if the reaction zone is used to define the flame position, then  $I_X$  vanishes. It is interesting to note that a term involving curvature was present in the Markstein model. Since  $I_X$  is always positive, our curvature term is always stabilizing, as anticipated in the Markstein model if the Markstein length  $l_M$  is positive. However, there is a second term at  $O(Pe^{-1})$  in (4.53) which may be either negative or positive. To study the relative importance of the two terms we investigate the coefficient  $I_Y + C_{(1)}I_H - I_X$ . We find that it is relatively small for a wide range of parameters, so that the flame speed often depends more strongly on curvature than on flame stretch. This is in contrast to what is found in Matalon & Matkowsky (1982), where the flame speed depends on flame stretch alone. To be sure, the difference is small,  $O(Pe^{-1})$ . Though both results are correct, this difference is due to the different definitions of the flame position, which themselves differ by  $O(Pe^{-1})$ . It is not surprising that there is a difference in the flame speed relations corresponding to different flame positions since the flame speed is the speed of the discontinuity surface relative to the speed of the moving gas and the latter varies within the flame region on an  $O(Pe^{-1})$  length scale. Put another way, the Matalon–Matkowsky result can be obtained from the unified result in the near-equidiffusional limit, by Taylor expansion. Thus, the mass flux through the reaction surface depends on stretch alone, as in Matalon & Matkowsky (1982), while the mass flux at any other surface depends on both curvature and stretch.

In the near-equidiffusional limit the flame speed relation (4.53) may be written as  $m = 1 - Mr_\chi\chi - Mr_c2c$ , where  $Mr_\chi = CI_H + Pe^{-1}(I_Y - I_X)$  is the Markstein number for stretch and  $Mr_c = Pe^{-1}I_X$  is the Markstein number for curvature. The effect of stretch becomes increasingly important with growing  $C$ .

### 4.3. Strong flame speed variations ( $C = O(1)$ )

If the Lewis number differs from unity by  $O(1)$  and the Zeldovich number is large then  $C = Pe^{-1}Ze(1 - Le^{-1}) = O(1)$ . Substituting this into (4.52) and neglecting  $O(Pe^{-1})$  terms yields

$$(\partial/\partial t + \chi)(1/m) - Pe^{-1}\frac{I_\Delta}{I_H}\nabla_\perp^2(1/m) + Pe^{-1}\frac{I_{\nabla^2}}{I_H}m(\nabla_\perp(1/m))^2 + \frac{1}{CI_H}m \ln m = 0. \quad (4.55)$$

Note that the transverse coupling terms are retained, since they are  $O(1)$  for short-wave perturbations where  $\nabla_\perp^2(1/m) = O(Pe)$  and  $m(\nabla_\perp(1/m))^2 = O(Pe)$ . Note further that  $O(Pe^{-1})$  terms have been omitted, so that  $m$  represents the leading-order mass flux. Higher-order terms cannot be obtained from (4.52) for  $C = O(1)$ . In this case the leading-order enthalpy equation yields  $H_{r(0)} = 0$ , which does not provide any information about  $m$ . The leading-order concentration equation yields the reaction rate  $W_{r(0)}$  as a function of  $H_{r(1)}$  and  $m_{(0)}$ . Therefore, in order to calculate the leading-order mass flux we would need to consider the enthalpy equation at  $O(Pe^{-1})$ . The concentration equation at  $O(Pe^{-1})$  yields the reaction rate  $W_{r(1)}$  as a function of  $H_{r(2)}$  and  $m_{(1)}$ . Therefore, perturbative corrections of  $m$  can only be obtained after solving the enthalpy equation at  $O(Pe^{-2})$ , which has not been done here.

If we were to ignore the effect of short waves, i.e. if we were to restrict the analysis to flame front corrugations which have an  $O(1)$  length scale, then the surface Laplacian and the square of the gradient in (4.54) become negligible and we recover the time-dependent flame speed relation of Sivashinsky (1976):

$$(\partial/\partial t + \chi)(1/m) + (CI_H)^{-1}m \ln m = 0. \quad (4.56)$$

The flame speed relation (4.54) represents a generalization of the flame speed relation of Sivashinsky (1976) and accounts for the coupling of neighbouring flame elements which damps short-wave corrugations of the flame.

#### 4.4. Moderate flame speed variations ( $C = O(Pe^{-1/2})$ )

For near-equidiffusional flames the flame speed is unity at leading order, so that the time-derivative term, which is present when  $C = O(1)$  or  $Le - 1 = O(1)$ , becomes negligibly small and drops out of the flame speed relation. Recall that this term was dismissed by Sivashinsky due to stability considerations. Here, we discuss an intermediate limit which reduces to the result of Matalon & Matkowsky (1982) as the Lewis number approaches unity, but which still contains the time-derivative term as well as the nonlinearity of Sivashinsky's result, though it does not require consideration of terms  $O(Pe^{-2})$ .

Let  $C = Pe^{-1}Ze(1 - Le^{-1}) = O(Pe^{-1/2})$ , i.e.  $C = Pe^{-1/2}C_{(1/2)}$  where  $C_{(1/2)}$  is  $O(1)$ , and expand in powers of  $Pe^{-1/2}$  so that

$$m \sim m_{(0)} + Pe^{-1/2}m_{(1/2)} + Pe^{-1}m_{(1)} + \dots \quad (4.57)$$

Now the flame speed relation (4.52) yields

$$m = 1 - Pe^{-1/2}C_{(1/2)}I_H\chi - Pe^{-1}\left(2cI_X + (I_Y - I_X)\chi + (C_{(1/2)}I_H)^2 \times \left(\frac{\partial\chi}{\partial t} - \frac{I_\Delta}{I_H}Pe^{-1}\nabla_\perp^2\chi + \frac{3}{2}\chi^2\right)\right) + o(Pe^{-1}), \quad (4.58)$$

where the transverse diffusion term is retained since  $Pe^{-1}\nabla_\perp^2\chi$  is  $O(1)$  for short-wave perturbations. Clearly, this equation has properties which were present in the limits previously considered. In particular, if  $C_{(1/2)}$  becomes small, so that  $C_{(1/2)} = O(Pe^{-1/2})$  then the nonlinear term and the time-derivative term become negligible and the  $O(Pe^{-1/2})$  term becomes  $O(Pe^{-1})$ , so that we recover the result of Matalon–Matkowsky (4.53). Similarly, if we let  $C$  become small in (4.54) we recover the  $O(Pe^{-1/2})$  term in (4.57), and the terms containing  $I_H$  at  $O(Pe^{-1})$ . In (4.57) the time derivative is present as is the curvature term. In contrast to (4.53), the flame speed relation (4.57) contains the time derivative which may result in the well-known pulsating instability. Finally, the nonlinear term  $\sim \chi^2$  leads to symmetry breaking, i.e. positive and negative stretch have opposite effects on the flame speed. This is a well-known feature. In particular, for cellular flames it is known that curvature is much stronger at the cold crests than it is at the hot cell centres, which is a manifestation of this asymmetry. The transverse diffusion term  $\nabla_\perp^2\chi$  results in the coupling of neighbouring flame elements.

It should also be noted that for flames with  $C = O(Pe^{-1/2})$  subjected to moderately large flame stretch,  $\chi = Pe^{1/2}\chi_{(-1/2)}$  where  $\chi_{(-1/2)} = O(1)$ , the unified flame speed relation (4.52) reduces to the stationary form of equation (4.54),

$$C_{(1/2)}I_H\chi_{(-1/2)} + m^2 \ln m = 0 + o(1), \quad (4.59)$$

which is the stationary relation of Sivashinsky (1976). The transverse diffusion terms are  $O(Pe^{-3/2})$  and thus are neglected. An illustrative example where strong stretch is relevant is the Bunsen flame. In a Bunsen flame the gas speed in the fresh mixture is above the adiabatic flame speed, so that the flame adjusts and forms a cone. Suppose we have a stable flame with a closed tip. At the tip the flame is normal to the flow direction, and it is required to propagate at a speed which is well above the adiabatic flame speed. The flame may adjust by a strong curvature and thus a strong flame stretch.

## 5. Conclusions

Darrieus and Landau proposed a model that describes a premixed flame as a gasdynamic discontinuity which propagates at a given flame speed, whose mass and momentum are continuous across the discontinuity, and showed that uniformly propagating planar flames governed by this model are unconditionally unstable. Since then there have been numerous attempts to both phenomenologically propose and analytically derive improved models that better explain the behaviour of flames. Among the analytically derived approaches, two separate and distinct cases have been considered, namely Lewis numbers close to unity and Lewis numbers bounded away from unity. An approach that simultaneously covers both cases has not been presented. Furthermore, no theory exists that describes the large-wavenumber cutoff of the pulsating instability for Lewis numbers greater than unity when  $O(1)$  thermal expansion is present.

In this paper we derived a unified model which is valid for arbitrary  $Le$ . It captures all the instabilities and exhibits the large-wavenumber cutoff for each. The model includes the effects of transverse diffusion, which is not present in earlier theories.

Our model consists of the incompressible Navier–Stokes equations in both the unburned and burned mixtures, the jump conditions (3.50)–(3.52) relating the fluid fields on the two sides of the flame surface, and the flame speed relation (4.52). The density ahead of and behind the flame surface is constant. The expressions for the jump conditions and the flame speed relation depend on the precise location of the discontinuity surface within the flame structure. Defining the flame position by a density integral (3.41) yields vanishing excess surface mass, leading to continuity of the mass flux across the flame. Continuity of the mass flux also simplifies the jump conditions substantially and allows for simple physical interpretation. Compressibility effects within the flame structure result in an additional pressure jump which is proportional to curvature, and thus physically may be interpreted as an analogue of surface tension. We refer to the term  $-Pe^{-1}mI_\sigma$  as surface compression since its sign is opposite to that of surface tension. Variations of the surface compression along the flame result in tangential forces which act on the flow.

The unified flame speed relation (4.53) is a nonlinear partial differential equation, containing a time derivative, a transverse diffusion term, and a nonlinear term involving the transverse spatial gradient, i.e. the flame requires a characteristic time to adjust to new conditions and neighbouring flame elements cannot propagate at uncorrelated flame speeds. Neighbouring flame elements are able to communicate with one another via the transverse diffusion term and the nonlinear term. If we restrict consideration to  $O(1)$  variations along the flame, i.e. if we ignore the effect of short-wavelength variations, the unified flame speed relation reduces to the flame speed relations previously derived by Sivashinsky (1976), and Matalon & Matkowsky (1982) in the appropriate limits. We also present a new intermediate case. The jump

conditions (3.50)–(3.52) are valid for arbitrary chemistry. The flame speed relation (4.53) is valid for flames with thin reaction zones.

Our model is presented in coordinate-free form, which in particular is suitable for use in numerical calculations employing either the level set method (see Sethian 1996; Osher & Fedkiw 2002), where a partial differential equation for a scalar is introduced which measures the distance from the flame surface, or the G-equation where a partial differential equation for a phase function is introduced which determines the state of the mixture, i.e. burned or fresh. In both methods the speed of the propagating surface must be prescribed, which is the case for our model. Both methods are described in the book by Peters (2000). Both methods require continuity of mass flux across the flame, which is ensured by our definition of the flame location. We plan to implement numerical codes for the computation of flames based on our model in terms of these methods.

This paper is dedicated to Professor U. Müller on his retirement. This research was supported by NSF grant DMS 00-72491 and DFG grant SFB 606.

#### REFERENCES

- ARIS, R. 1989 *Vectors, Tensors, and the Basic Equations of Fluid Mechanics*. Dover.
- BARENBLATT, G. I., ZELDOVICH, Y. B. & ISTRATOV, A. G. 1962 On diffusional thermal instability of laminar flame. *Prikl. Mekh. Tekh. Fiz.* **2**, 21–26.
- CLASS, A. G., MATKOWSKY, B. J. & KLIMENKO, A. Y. 2003 Stability of planar flames as gasdynamic discontinuities. *J. Fluid Mech.* **491**, 51–63.
- CLAVIN, P. & WILLIAMS, F. A. 1982 Effects of molecular diffusion and of thermal expansion on the structure and dynamics of premixed flames in turbulent flows of large scales and low intensity. *J. Fluid. Mech.* **116**, 251–282.
- DARRIEUS, G. 1938, 1945 Propagation d'un front de flamme. Presented at *La Technique Moderne and Le Congrès de Mécanique Appliquée, Paris*.
- ECKHAUS, W. 1961 Theory of flame-front stability. *J. Fluid Mech.* **10**, 80–100.
- GIBBS, J. 1879 Abstract of “on the equilibrium of heterogeneous substances”. *Am. J. Sci.* **18** (3), 277–293; 371–387.
- GIBBS, J. W. 1876, 1878 On the equilibrium of heterogeneous substances. *Trans. Conn. Acad.* **3**, 108–248; 343–524.
- DE GOEY, L. P. H. & TEN THIJE BOONKAMP, J. H. M. 1999 A flamelet description of premixed flames and the relation with flame stretch. *Combust. Flame* **119**, 253–271.
- KARLOVITZ, B., DENNISTON, D. W., KNAPSCHAEFER, H. D. & WELLS, F. E. 1953 Studies on turbulent flames. *Fourth Symposium (Intl) on Combustion*, pp. 613–620. The Combustion Institute.
- KLIMENKO, A. Y. & CLASS, A. G. 2000 On premixed flames as gasdynamic discontinuities: A simple approach to derive their propagation speed. *Combust. Sci. Tech.* **160**, 25–37.
- KLIMENKO, A. Y. & CLASS, A. G. 2002 Propagation of nonstationary curved and stretched premixed flames with multistep reaction mechanisms. *Combust. Sci. Tech.* **174** (8), 1–43.
- LANDAU, L. D. 1944 On the theory of slow combustion. *Acta Physicochimica URSS* **19**, 77–85.
- MARKSTEIN, G. H. 1951 Experimental and theoretical studies of flame front stability. *J. Aero. Sci.* **18**, 199–209.
- MARKSTEIN, G. H. (Ed.) 1964 *Nonsteady Flame Propagation*. Pergamon.
- MATALON, M. & MATKOWSKY, B. J. 1982 Flames as gasdynamic discontinuities. *J. Fluid Mech.* **124**, 239–259.
- MATALON, M. & MATKOWSKY, B. J. 1984 On the stability of plane and curved flames. *SIAM J. Appl. Maths* **44**, 327–343.
- MATKOWSKY, B. J. & SIVASHINSKY, G. I. 1979 An asymptotic derivation of two models in flame theory associated with the constant density approximation. *SIAM J. Appl. Maths* **37**, 686–699.
- OSHER, S. & FEDKIW, R. 2002 *Level Set Methods and Dynamic Implicit Surfaces*. Springer.

- PELCE, P. & CLAVIN, P. 1982 Influence of hydrodynamics and diffusion upon the stability limits of laminar premixed flames. *J. Fluid Mech.* **124**, 219–237.
- PETERS, N. 2000 *Turbulent Combustion*. Cambridge University Press.
- SEARBY, G. & QUINARD, J. 1990 Direct and indirect measurements of markstein numbers of premixed flames. *Combust. Flame* **82** (3), 298–311.
- SETHIAN, J. A. 1996 *Level Set Methods*. Cambridge University Press.
- SIVASHINSKY, G. I. 1976 On a distorted flame front as a hydrodynamic discontinuity. *Acta Astronautica* **3**, 889–918.
- SIVASHINSKY, G. I. 1980 On flame propagation under conditions of stoichiometry. *SIAM J. Appl. Maths* **39**, 67–82.
- ZELDOVICH, Y. B., BARENBLATT, G. I., LIBROVICH, V. B. & MAKHVILADZE, G. M. 1985 *The Mathematical Theory of Combustion and Explosions*. New York: Consultants Bureau.